Density-functional-theory calculations of second-order magnetic properties

Thesis submitted for the degree of *Philosophiae Doctor*

by

Ola Berg Lutnæs

CTCC - Centre for Theoretical and Computational Chemistry
Department of Chemistry
Faculty of Mathematics and Natural Sciences
University of Oslo

Series of dissertations submitted to the
Faculty of Mathematics and Natural Sciences, University of Oslo
Nr. 873

ISSN 1501-7710

Cover: Inger Sandved Anfinsen.
Printed in Norway: AiT e-dit AS, Oslo, 2009.

Produced in co-operation with Unipub AS.
The thesis is produced by Unipub AS merely in connection with the
thesis defence. Kindly direct all inquiries regarding the thesis to the copyright
holder or the unit which grants the doctorate.

Unipub AS is owned by
The University Foundation for Student Life (SiO)

Acknowledgments

This thesis is a result of my work at the University of Oslo for a period of six years from 2003–2009. During this time, I have also had a half year stay at the University of Durham, UK.

First, I would like to thank my supervisors Trygve Helgaker and David J. Tozer for kind help and inspiring discussions.

Indeed, new knowledge is not best acquired in solitude. I would like to thank all my close collaborators and colleagues during my PhD studies, in particular, Michał Jaszuński, Torgeir Ruden, Dave Wilson, Andy Teale, Kenneth Ruud, Alessandro Soncini, Kjetil Jacobsen, Pawel Sałek, Jonas Juselius, Vebjørn Bakken, Erik Tellgren, Simen Reine, Francesca Iozzi, Andreas Krapp, Knut Fægri, Michael Peach, Tom Keal, Nick Handy, Chris Mohn, Harald Møllendal, Kai Lange, Seema Singh, Mette Nilsen, Pål Dahle and Søren Larsen for all help, support and discussions.

Trygve Helgaker has generously given me financial support from his research grants for travels to several conferences and also for my half year stay in Durham. I have also received financial support from NorFa to participate at the European Summerschool in Quantum Chemistry 2003 (ESQC-03), and also the Winter School in Theoretical Chemistry, Helsinki, 2003. I thank Durham University and David Tozer for letting me a pleasant and motivating visit in Durham. I thank the Chemistry Department at the University of Oslo for releasing me from teaching duties during that stay.

List of Papers

I *The performance of hybrid density functional theory for the calculation of indirect nuclear spin–spin coupling constants in substituted hydrocarbons*
O. B. Lutnæs, T. A. Ruden and T. Helgaker
Magnetic Resonance in Chemistry, Volume 42, Pages S117-S127, 2004

II *Vibrational corrections to indirect nuclear spin–spin coupling constants calculated by density-functional theory*
T. A. Ruden, O. B. Lutnæs, T. Helgaker and K. Ruud
Journal of Chemical Physics, Volume 118, Pages 9572-9581, 2003

III *Assessment of a Coulomb-attenuated exchange-correlation energy functional*
M. J. G. Peach, T. Helgaker, P. Sałek, T. W. Keal, O. B. Lutnæs, D. J. Tozer and N. C. Handy
Physical Chemistry Chemical Physics, Volume 8, Pages 558-562, 2006

IV *Density-functional and coupled-cluster singles-and-doubles calculations of the nuclear shielding and indirect nuclear spin–spin coupling constants of o-benzyne*
T. Helgaker, O. B. Lutnæs and M. Jaszuński
Journal of Chemical Theory and Computation, Volume 3, Pages 86-94, 2007

V *Density-functional calculations of the nuclear magnetic shielding and indirect nuclear spin–spin coupling constants of three isomers of C_{20}*
O. B. Lutnæs, T. Helgaker and M. Jaszuński
Molecular Physics, Volume 106, Pages 2357-2365, 2008

VI *The rotational g tensor as a benchmark for ab initio molecular property calculations*
C. E. Mohn, D. J. D. Wilson, O. B. Lutnæs, T. Helgaker and K. Ruud
Advances in Quantum Chemistry, Volume 50, Pages 77-90, 2005

VII *Rotational g tensors calculated using hybrid exchange-correlation functionals with the optimized effective potential approach*
O. B. Lutnæs, A. M. Teale, T. Helgaker and D. J. Tozer
Journal of Chemical Theory and Computation, Volume 2, Pages 827-834, 2006

VIII *Benchmarking Density Functional Theory Calculations of Rotational g-tensors and Magnetizabilities using accurate Coupled Cluster Calculations*
O. B. Lutnæs, A. M. Teale, T. Helgaker, D. J. Tozer, K. Ruud and J. Gauss
Manuscript in preparation.

Contents

Chapter 1

The Molecular Energy

In this Chapter, the relevant theory for the evaluation of the molecular electronic energy in quantum chemistry is introduced in order to define a reference for further discussions. A thorough description of quantum-chemistry models and the underlying quantum-mechanics theory can be found in textbooks [1, 2, 3].

First, the Schrödinger equation is introduced in Section 1.1 followed by the Born–Oppenheimer approximation in Section 1.2 and the variation principle in Section 1.3. Expansions of approximate wave functions in Slater determinants are described in Section 1.4 including the orbital approximation, Hartree–Fock theory and coupled-cluster theory.

We then move on to density-functional theory (DFT) in Section 1.5, which is the quantum chemical method of main interest in this work. Its foundation on the Hohenberg–Kohn theorems is described before the practical DFT implementation of Kohn–Sham theory. Some of the main classes of Kohn–Sham density functionals are then described. Then, Kohn–Sham DFT effective potentials are treated before finally, current-density-functional theory (CDFT) is discussed.

1.1 The Schrödinger Equation

The theory of quantum mechanics is one of the most well-tested theories in science and it has not yet been proven wrong. The mathematical machinery of the theory may be represented by the time-independent non-relativistic Schrödinger equation

$$\hat{H}\psi = E\psi \tag{1.1}$$

which describes the stationary states of a system of particles in the absence of time-dependent fields. Here, the operator $\hat{H}$ is the Hamiltonian, which for an isolated

molecule reads (in atomic units)

$$\hat{H} = -\frac{1}{2}\sum_i \nabla_i^2 - \frac{1}{2}\sum_K \frac{\nabla_K^2}{M_K} - \sum_{iK} \frac{Z_K}{r_{iK}} + \sum_{i<j} \frac{1}{r_{ij}} + \sum_{K<L} \frac{Z_K Z_L}{r_{KL}}. \tag{1.2}$$

The sums over i and j run through all the electrons and the sums over K and L run through all the nuclei of the molecule, r_{ab} denotes the distance between the particles a and b and Z_L is the charge and M_L is the mass of nucleus L. The five terms in the Hamiltonian operator Eq.(1.2) represent the electronic kinetic, the nuclear kinetic, the electron–nucleus attraction, the electron–electron repulsion and the nucleus–nucleus repulsion energies, respectively.

The function Ψ in Eq.(1.1) is the wave function which is dependent on all the space and spin coordinates of all the particles in the system. It contains all the information we can possibly have about the system. The wave function is subject to several constraints. It must be normalizable, differentiable and single-valued. The Pauli-principle imposes that the wave function of fermions should be antisymmetric with respect to interchange of two particle coordinates.

Finally, in Eq.(1.1), E is the total energy of the system. Quantization arises from the fact that the Schrödinger equation only has a distinct set of valid solutions with corresponding wave functions (states) and energies. The state with lowest energy is called the ground state, Ψ_0, and its energy is the ground-state energy, E_0.

The Schrödinger equation does not include a relativistic treatment of the particles. Including the theory of relativity in the quantum-mechanical treatment of the particles leads to the more complete Dirac equation, see for example Dyall and Fægri [4]. Relativistic effects are however small for molecules considered in this thesis, considering only light atoms from the first and second rows of the periodic table, and we may to a good approximation employ the Schrödinger equation. Further approximations are introduced through the Born–Oppenheimer approximation in the next section.

1.2 The Born–Oppenheimer Approximation

The Born–Oppenheimer approximation is widely used in quantum chemical calculations. The validity of the Born–Oppenheimer approximation is based on the fact that the nuclei are much heavier and move much slower than the electrons. This means that to a good approximation, the nuclei can be considered to have a fixed geometry since the electrons will instantaneously adapt to every nuclear configuration.

Fixing the nuclei, which may be achieved by considering the nuclear mass to be infinitely large, results in a considerably simplified Hamiltonian operator Eq.(1.2). The kinetic energy operator of the nuclei vanish due to the presence of the nuclear mass in the denominator, and since the nuclear coordinates become parameters, the nuclear repulsion potential energy is reduced to a constant V_{nuc}, and the electron-nucleus attraction potential becomes only parametrically dependent on the nuclear coordinates

$$\hat{H}_{\text{el}} = -\frac{1}{2}\sum_i \nabla_i^2 - \sum_{iK}\frac{Z_K}{r_{iK}} + \sum_{i<j}\frac{1}{r_{ij}} + V_{\text{nuc}}. \tag{1.3}$$

The Schrödinger equation Eq.(1.1), together with the Hamiltonian Eq.(1.3) can now be considered an electronic Schrödinger equation—it describes the states of the collection of electrons moving in the potential set up by the spatially fixed nuclei. The electronic energy as a function of the nuclear coordinates is termed the potential energy surface of the molecule.

1.3 The Variation Principle

The energy of an approximate wave function, not necessarily an eigenfunction of the Hamiltonian operator, can be evaluated as the expectation value

$$E = \langle \hat{H} \rangle = \frac{\langle \psi | \hat{H} | \psi \rangle}{\langle \psi | \psi \rangle} \tag{1.4}$$

where bracket notation is used for the integrals,

$$\langle a|b\rangle = \int a^* b \, \mathrm{d}\boldsymbol{\tau} \tag{1.5}$$

$$\langle a|\hat{O}|b\rangle = \int a^* \hat{O} b \, \mathrm{d}\boldsymbol{\tau} \tag{1.6}$$

where a and b are functions and $\hat{O}$ is an operator.

The variation principle states that all approximate wave functions have an energy expectation value that is higher than that of the true ground-state wave function.

$$E_0 = \frac{\langle \psi_0 | \hat{H} | \psi_0 \rangle}{\langle \psi_0 | \psi_0 \rangle} \leq \frac{\langle \psi | \hat{H} | \psi \rangle}{\langle \psi | \psi \rangle} \tag{1.7}$$

where the zero subscript denotes a ground state. Thus, among approximate wave functions, the variation principle can be used as a guide — the best approximation to the ground-state wave function is the approximate wave function that has the lowest energy. The minimum energy of an approximate wave function dependent on some

parameters $\boldsymbol{\lambda}$ is then made a stationary point with respect to those parameters, that is

$$\left.\frac{\mathrm{d}E}{\mathrm{d}\boldsymbol{\lambda}}\right|_{\boldsymbol{\lambda}=\boldsymbol{\lambda}_0} = 0 \tag{1.8}$$

for the optimized parameters $\boldsymbol{\lambda}_0$.

1.4 Approximate Wave Functions

Exact analytic solution of the Schrödinger equation Eq.(1.1) is only possible for the simplest systems, for example the hydrogen atom. To solve problems of chemical interest, it is necessary to introduce approximate wave functions. We may divide the approximate wave functions into two classes. Variational wave functions containing parameters to be determined by minimization of the energy according to the variation principle and non-variational wave functions where the parameters are determined in some other manner without the use of the variation principle.

Here, some of the approximate wave functions used in quantum chemistry will be presented. The orbital approximation is introduced in Section 1.4.1 before the Hartree–Fock theory and coupled-cluster theory are presented in Section 1.4.2 and 1.4.3, respectively.

1.4.1 The Orbital Approximation

In the orbital approximation, wave functions are approximated using *molecular orbitals*, that is one-electron functions dependent on the coordinates of only one particle. The molecular orbitals ϕ are usually constructed in a basis of known functions

$$\phi_i(\mathbf{r}) = \sum_\alpha c_{i\alpha}\chi_\alpha(\mathbf{r}), \tag{1.9}$$

where the sum runs over the number of basis functions, $c_{i\alpha}$ are expansion coefficients and $\chi_\alpha(\mathbf{r})$ constitute a set of functions known as the basis set. Several choices can be made for the functional form of the basis set. In this work we use atom-centered Gaussian functions

$$\chi_\alpha(\mathbf{r}) \;=\; MP(x_\alpha, y_\alpha, z_\alpha)\exp\left[-\mu\left|\mathbf{r}_\alpha\right|^2\right] \tag{1.10}$$

Here, μ is a constant (the *exponent* of the basis function), M is a normalization constant, $\mathbf{r}_\alpha$ is the distance vector from the center of the basis function to the point $\mathbf{r}$ and P is a polynomial in the components of $\mathbf{r}_\alpha$ (for spherical Gaussian functions, P is a solid harmonic function S_{lm}).

1.4.2 Hartree–Fock theory

In Hartree–Fock theory, the wave function is approximated as a Slater determinant

$$\psi^{\mathrm{HF}} = \Phi\left(\mathbf{r}_1, \mathbf{r}_2, \ldots, \mathbf{r}_N\right) = \begin{vmatrix} \phi_1\left(\mathbf{r_1}\right) & \phi_2\left(\mathbf{r_1}\right) & \ldots & \phi_N\left(\mathbf{r_1}\right) \\ \phi_1\left(\mathbf{r_2}\right) & \phi_2\left(\mathbf{r_2}\right) & \ldots & \phi_N\left(\mathbf{r_2}\right) \\ \vdots & \vdots & \ddots & \vdots \\ \phi_1\left(\mathbf{r_N}\right) & \phi_2\left(\mathbf{r_N}\right) & \ldots & \phi_N\left(\mathbf{r_N}\right) \end{vmatrix} \tag{1.11}$$

where N is the number of electrons. The Slater determinant represents the simplest form of an antisymmetrized wave function constructed from a product of molecular orbitals. The Slater determinant satisfies the Pauli principle.

Applying the variation principle Eq.(1.7) to the Hartree–Fock wave function, minimizing the energy with respect to the variational parameters $c_{i\alpha}$ under the constraint that the molecular orbitals are orthonormal, the minimum energy is found by solving a set of one-electron equations, the Hartree–Fock equations

$$\hat{f}_i \phi_i = \epsilon_i \phi_i \tag{1.12}$$

where the Fock operator is

$$\hat{f}_i = -\frac{1}{2}\nabla_i^2 - \sum_K \frac{Z_K}{r_{iK}} + \sum_j^N \left(J_{ij} - K_{ij}\right) \tag{1.13}$$

and ϵ_i are the orbital energies. The three terms in the Fock operator Eq.(1.13) represent the kinetic energy, the nuclear attraction energy and an effective electron–electron repulsion energy, respectively, for the electron in ϕ_i. The effective electron–electron repulsion operator consists of the classical Coulomb operator J and the quantum-mechanical exchange operator K

$$J_{ij} = \int \frac{\phi_j^*\left(\mathbf{r}'\right)\phi_j\left(\mathbf{r}'\right)}{\left|\mathbf{r}' - \mathbf{r}_i\right|}\,\mathrm{d}\mathbf{r}' \tag{1.14}$$

$$K_{ij} = \int \frac{\phi_j^*\left(\mathbf{r}'\right)\hat{P}_{ij}\phi_j\left(\mathbf{r}'\right)}{\left|\mathbf{r}' - \mathbf{r}_i\right|}\,\mathrm{d}\mathbf{r}' \tag{1.15}$$

where $\hat{P}_{ij}$ is a permutation operator swapping i and j. Note that due to the permutation operator, the exchange potential is not a purely multiplicative potential.

In solving the Hartree–Fock equations, an iterative approach must be used as the Fock operator itself contains the solution—that is, the orbitals. This iterative procedure may be the self-consistent-field (SCF) method:

1. Input a set of trial orbitals
2. Construct the Fock operator from the orbitals
3. Solve the Hartree-Fock equations to give a new set of orbitals
4. Iterate from 2 till the orbitals do not change from last iteration (the orbitals are self consistent)

The final N orbitals of lowest energy ϵ_i are occupied in the Slater determinant. The remaining non-occupied orbitals are termed virtual orbitals.

The Hartree–Fock wave function is also termed the mean-field approximation pointing out that in this model, the Coulomb potential in Eq.(1.13) represents the time-averaged classical electrostatic potential set up by the other electrons. Thus, the Hartree–Fock model does not account for correlated motion of the electrons due to instantaneous Coulomb interactions.

Fermi-correlation arising from the antisymmetry of the wave function, is however included in the Hartree–Fock model. Fermi-correlation refers to the fact that two electrons of the same spin can not have the same positions since the Slater determinant wave function will then vanish. The correlation that is neglected in the Hartree–Fock model, is included in correlated models (although approximately in approximate methods) such as coupled-cluster theory which is described in the next section.

1.4.3 Coupled-Cluster Theory

Before describing coupled-cluster theory, we will take a detour to the full-configuration-interaction (FCI) model. A fully correlated and exact model can be obtained (within the completeness of the basis set) by extending the Hartree–Fock wave function in a linear expansion of all possible Slater determinants constructed from the occupied and virtual orbitals. This model is termed the FCI model and its wave function Ψ^{FCI} can be written

$$\Psi^{\mathrm{FCI}} = c_0\Phi_0 + \sum_{ia} c_{ia}\Phi_i^a + \sum_{ijab} c_{ijab}\Phi_{ij}^{ab} + \dots \tag{1.16}$$

The determinant Φ_0 is the reference determinant, possibly the Hartree–Fock ground state determinant, Φ_i^a are the set of singly virtually excited determinants (created by replacing an occupied orbital i with a virtual orbital a in Φ_0), Φ_{ij}^{ab} are the doubly excited determinants and so on. The coefficients c may be determined variationally to obtain the ground state FCI wave function, Ψ_0^{FCI}. The FCI expansion in Eq.(1.16)

quickly becomes very large and is intractable for all but the simplest molecular systems. Simplifying the FCI expansion by truncation at some virtual excitation level gives truncated CI wave functions. The truncated CI models do however not have the highly desirable property of size-extensivity—that is, the correct scaling of the model (and correlation energy) with increasing system size. For a discussion of size-extensivity, see the review of Bartlett [5].

Coupled-cluster theory provides a means of including correlation in a truncated form without the loss of size-extensivity. The coupled-cluster wave function can be written in the exponential ansatz as

$$\Psi^{\mathrm{CC}} = \exp\left(\hat{T}\right)\Phi_0 \tag{1.17}$$

where Φ_0 is a reference Slater determinant, and the cluster operator

$$\hat{T} = \hat{T}_1 + \hat{T}_2 + \ldots + \hat{T}_N \tag{1.18}$$

generates all excited determinants, the singly excited determinants through $\hat{T}_1$, the doubly excited determinants through $\hat{T}_2$ and so on. For example,

$$\hat{T}_1 = \sum_{ia} t_i^a \hat{\kappa}_{ia}, \tag{1.19}$$

where $\hat{\kappa}_{ia}$ generates a singly excited determinant Φ_i^a. The operators in Eq.(1.18) contain excitation amplitudes t_i^a, $t_{ij}^{ab}\ldots$ that are determined non-variationally by solving the coupled-cluster amplitude equations. Truncating the cluster operator at $\hat{T}_2$ gives the coupled-cluster-singles-and-doubles (CCSD) model. Inclusion of also the $\hat{T}_3$ operator yields the coupled-cluster-singles-doubles-and-triples (CCSDT) model. It is also possible to treat the triples contribution using perturbation theory giving the CCSD(T) model.

It is worth noting that contrary to truncated CI wave functions, coupled-cluster wave functions using a truncation of Eq.(1.18) contain contributions from all excited determinants in Eq.(1.16). For CCSD, this can be seen from the expansion of the exponential of the cluster operator in Eq.(1.17)

$$\exp\left(\hat{T}\right) = 1 + \left(\hat{T}_1 + \hat{T}_2\right) + \frac{1}{2}\left(\hat{T}_1 + \hat{T}_2\right)^2 + \ldots \tag{1.20}$$

where $\hat{T}$ has been truncated at $\hat{T}_2$—for example, the resulting $\frac{1}{2}\hat{T}_2\hat{T}_2$ term from the last term of Eq.(1.20) will give rise to quadruple excitations.

1.5 Density-Functional Theory

In density-functional theory (DFT), the electron density, $\rho(\mathbf{r})$, replaces the wave function as the identity that contains the information about the system. Although DFT because of this may appear to be a theory separate from wave-function methods described in the preceding sections, the proof of the validity of DFT, just as the wave-function methods, is rooted in the theory of quantum mechanics. In Section 1.5.1, these proofs, called the Hohenberg–Kohn theorems are described.

The obvious advantage of working with the electron density instead of the wave function is that the electron density is a much simpler function. It is only dependent on three spatial coordinates, whereas the wave function is dependent on the three spatial coordinates of all the electrons. Intuitively therefore, the solution of quantum chemical problems should be simpler within DFT than within wave-function methods. However, to obtain accurate results, DFT must today resort to the Kohn–Sham scheme using molecular orbitals, a Slater determinant "wave function" and the solution of one-electron equations using SCF procedures similar to Hartree–Fock theory. Still the Kohn–Sham method has advantages over Hartree–Fock theory as it includes correlation of the electrons, and in principle, the correlation description is exact. For practical calculations however, the Kohn–Sham DFT must be approximated since one of the ingredients, the exchange–correlation functional, is not completely known. Approximate exchange–correlation functionals lead to approximate descriptions of the electron correlation in DFT applications. The development of more accurate exchange–correlation Kohn–Sham DFT functionals is a major research interest in theoretical chemistry.

Following the Hohenberg–Kohn theorems, we outline Kohn–Sham theory in Section 1.5.2 followed by a qualitative description of approximations to the exchange–correlation functionals used for Kohn–Sham DFT in Section 1.5.3. In Section 1.5.4, the optimized effective potential (OEP) of a functional is described before constrained-search methods to obtain Kohn–Sham potentials from input electron densities are treated in Section 1.5.5. Finally, in Section 1.5.6, current-density-functional theory is discussed.

1.5.1 The Hohenberg–Kohn Theorems

The theoretical foundation for DFT was provided by Hohenberg and Kohn and consists of the two Hohenberg–Kohn theorems [6]. It is important to note that the Hohenberg–Kohn theorems are only valid for the set of physical (v-representable) elec-

tron densities—that is, electron densities associated with the ground-state wave function from the solution of the Schrödinger equation using some potential v. Since it is not possible to determine a priori whether an electron density is v-representable or not, this restriction is a problem. It is, however, possible to generalize the Hohenberg–Kohn theorems to overcome these difficulties [7, 8].

Consider the electronic Hamiltonian Eq.(1.3). For N electrons this Hamiltonian is made distinct by the form of the nuclear potential set up by the nuclear charges (the nuclear potential is a special case of a more general multiplicative external potential v_{ext}). Therefore, also the wave function as the solution to Eq.(1.1) is made distinct by the external potential. The first Hohenberg–Kohn theorem is a proof that there is a one to one mapping between the external potential v_{ext} (apart from a trivial constant potential) and the non-degenerate ground-state electron density. Consequently, the ground-state electron density determines the external potential which in turn determines the wave function of the system and all its properties including the energy. The ground-state energy can then be written exactly as a functional of the electron density, $E = E[\rho]$. Hohenberg and Kohn then split up the energy functional in two parts

$$E[\rho] = F[\rho] + \int \rho v_{\text{ext}} \, \mathrm{d}\mathbf{r} \tag{1.21}$$

where the functional F is universal and contains the electron kinetic and repulsion energy, T and V_{ee}

$$F[\rho] = T[\rho] + V_{\text{ee}}[\rho] \tag{1.22}$$

and the last term in Eq.(1.21) is system specific, dependent on the external potential.

The second Hohenberg–Kohn theorem establishes the validity of the variation principle for DFT. That is, given the exact form of the energy functional, any approximate electron density will give an energy that is higher than that for the exact ground-state electron density.

$$E_0 = E[\rho_0] \leq E[\rho] \tag{1.23}$$

where the equality only holds when the approximate density ρ is equal to the ground state density ρ_0.

1.5.2 Kohn–Sham Theory

It is difficult to find an accurate functional for the kinetic energy $T[\rho]$ using the electron density explicitly as the basic variable. To circumvent this problem, Kohn and Sham set up a theory based on a fictitious system of non-interacting electrons [9]. In this

case, the Schrödinger equation Eq.(1.1) can be solved exactly when the wave function is expressed as a single Slater determinant Eq.(1.11) (termed the Kohn–Sham determinant in Kohn–Sham DFT). The electrons are further assumed to move in an effective potential, v_{eff}, constructed such that the electron density becomes equal to the exact electron density for interacting electrons. The electron density is expressed as the sum of squares of the occupied orbitals in the Kohn–Sham determinant

$$\rho = \sum_{i}^{N} \phi_i^* \phi_i \tag{1.24}$$

N being the number of electrons. The exact energy functional Eq.(1.21) can now be written

$$E\left[\rho, \phi\right] = F\left[\rho, \phi\right] + \int \rho v_{\text{ext}} \, \mathrm{d}\mathbf{r} = T_{\text{S}}\left[\phi\right] + J\left[\rho\right] + E_{\text{xc}}\left[\rho\right] + \int \rho v_{\text{ext}} \, \mathrm{d}\mathbf{r} \tag{1.25}$$

where T_{S} is the approximate kinetic energy evaluated from the system of non-interacting electrons as an expectation value of the kinetic energy operator

$$T_{\text{S}}\left[\phi\right] = -\frac{1}{2}\langle \Phi \left| \nabla^2 \right| \Phi \rangle = -\frac{1}{2}\sum_{i}^{N} \langle \phi_i \left| \nabla^2 \right| \phi_i \rangle, \tag{1.26}$$

J is the Coulomb repulsion part of the electron–electron interaction

$$J\left[\rho\right] = \int\int \frac{\rho\left(\mathbf{r}\right)\rho\left(\mathbf{r}'\right)}{\left|\mathbf{r} - \mathbf{r}'\right|} \, \mathrm{d}\mathbf{r}\mathrm{d}\mathbf{r}' \tag{1.27}$$

and E_{xc} is the exchange–correlation energy which by definition contains the remaining parts of the kinetic and electron–electron repulsion energies

$$E_{\text{xc}} = \left(T - T_{\text{S}}\right) + \left(V_{\text{ee}} - J\right). \tag{1.28}$$

Here, the first term on the right is the difference between the exact kinetic energy T and the approximate T_{S}, and the second term is the difference between the exact electron–electron repulsion V_{ee} and the Coulomb repulsion J (due to the the neglect of exchange energy and the electron self repulsion in Eq.(1.27)). As a result of this definition of E_{xc}, the energy expression Eq.(1.25) is exact.

The orbitals are obtained by solving a set of one-electron equations, the Kohn–Sham equations

$$\hat{f}_{\text{KS}}\phi_i = \epsilon_i \phi_i. \tag{1.29}$$

The orthogonal orbitals ϕ_i are occupied in the Kohn–Sham determinant according to the aufbau principle, the eigenvalues ϵ_i being the orbital energies. The Kohn–Sham-operator is

$$\hat{f}_{\text{KS}} = -\frac{1}{2}\nabla^2 + v_{\text{eff}} \tag{1.30}$$

where v_{eff} is an effective multiplicative potential which can be evaluated as the functional derivative of the non-kinetic energy terms in Eq.(1.25). It is

$$v_{\text{eff}}(\mathbf{r}) = v_{\text{ext}}(\mathbf{r}) + \int \frac{\rho(\mathbf{r}')}{|\mathbf{r} - \mathbf{r}'|} \, \mathrm{d}\mathbf{r}' + v_{\text{xc}}(\mathbf{r}) \,. \tag{1.31}$$

where the exchange–correlation potential v_{xc} is defined as the functional derivative of the exchange–correlation energy with respect to the electron density

$$v_{\text{xc}} = \frac{\delta E_{\text{xc}}}{\delta \rho}. \tag{1.32}$$

In Hartree–Fock theory, each electron can be said to move in the average electrostatic potential set up by the other electrons. Therefore, the form of the Fock-operator Eq.(1.13) is equal for all the virtual orbitals where the potential contains all electrons, but different for each occupied orbital as the potential contain only the repulsion from the other electrons. In Kohn–Sham DFT the situation is different. Here the multiplicative potential v_{eff} is equal in all the Kohn–Sham equations, both for occupied and virtual orbitals. The Kohn–Sham equations therefore treat all the electrons in a physically appealing indistinguishable form.

1.5.3 Functionals

Numerous approximations to the exchange–correlation energy Eq.(1.28) have been developed. In this section, we will describe the functionals used in this work. A more general exposition on functionals and their developments can be found for example in Refs. [10, 11].

First, let us note that it is common to split the exchange–correlation energy functional into a functional of exchange (X) and correlation (C) separately

$$E_{\text{xc}} = E_{\text{X}} + E_{\text{C}} \tag{1.33}$$

The exchange–correlation functionals may depend on several variables, for example, the electron density, the gradient of the electron density and also different functional forms constructed from the Kohn–Sham orbitals

$$E_{\text{xc}} = E_{\text{xc}}[\rho, \nabla\rho, \phi] \tag{1.34}$$

The density and orbital variables are often separated into two variables, one for each type of electron spin, α and β (i.e. $\rho \rightarrow \rho_\alpha, \rho_\beta$). Depending on which variables are contained in the exchange-correlation functional, the functionals are separated into

different classes. The local density approximation (LDA) is dependent only on the electron density. The generalized gradient approximations (GGA) are also dependent on the density gradient. In this class we find the functionals KT1, KT2, BLYP and PBE. The hybrid functionals include a proportion of Hartree–Fock-exchange

$$E_{\mathrm{X}}^{\mathrm{HF}} = \sum_{ij} \int \int \frac{\phi_i^* (\mathbf{r}) \, \phi_i (\mathbf{r}') \, \phi_j (\mathbf{r}) \, \phi_j^* (\mathbf{r}')}{|\mathbf{r}' - \mathbf{r}|} \, \mathrm{d}\mathbf{r}\mathrm{d}\mathbf{r}' \tag{1.35}$$

using the Hartree–Fock exchange energy expression. Functionals of this type are B3LYP, PBE0, B97-2, B97-3 and CAM-B3LYP.

Other orbital-dependent variables used in exchange–correlation energy functionals include the paramagnetic current density [12, 13] (see also Section 1.5.6)

$$\mathbf{j}_{\mathrm{p}} = -\frac{\mathrm{i}}{2} \sum_i \left[\phi_i^* \nabla \phi_i - (\nabla \phi_i^*) \, \phi_i \right] \tag{1.36}$$

and the kinetic energy density [14, 15]

$$\tau = \sum_i \frac{1}{2} \left| \nabla \phi_i \right|^2 \tag{1.37}$$

where the sums in Eq.(1.36) and Eq.(1.37) run over the occupied orbitals. A set of relevant functionals are shortly described in the next sections.

LDA

The local density approximation (LDA) is based on the properties of a uniform electron gas and is dependent on the electron density only. In this case the exchange energy can be found exactly. It is [16]

$$E_{\mathrm{X}}^{\mathrm{LDA}} [\rho] = -\frac{3}{4} \left(\frac{3}{\pi} \right)^{(1/3)} \int \rho^{4/3} (\mathbf{r}) \, \mathrm{d}\mathbf{r}. \tag{1.38}$$

The correlation energy E_{C}, has been parameterized by Vosko, Wilk and Nusair (WVN) [17] to fit the exact high and low density limits to the correlation energy in addition to Monte Carlo simulation data by Ceperley and Alder [18].

BLYP

The BLYP functional is a GGA functional dependent on both the electron density and its gradient. BLYP consists of the Becke functional (B) [19] for exchange and the Lee–Yang–Parr functional (LYP) [20, 21] for correlation. The B exchange functional has the correct asymptotic behavior of the exchange potential $v_{\mathrm{X}} \rightarrow -\frac{1}{r}$ for large distances

and contains one empirical parameter fitted to exact exchange energies of noble gas atoms from Hartree–Fock calculations. The LYP correlation functional is based on the expression for the correlation energy developed by Colle and Salvetti [21] (expression in the electron density and the second-order reduced density matrix fitted to He atom) which has been reformulated into a functional dependent on the electron density and its second-order gradient.

PBE

The Perdew–Burke–Ernzerhof (PBE) functional is a GGA functional for both exchange and correlation [22]. The main idea behind the functional development is to satisfy exact conditions on the exchange and correlation functionals important for the energy evaluation rather that fitting parameters to empirical data. The functional contains no empirical parameters except the LDA correlation parameters of VWN.

KT1 and KT2

The KT1 and KT2 functionals were developed by Keal and Tozer [23] and the initial emphasis was to reproduce high quality Kohn–Sham exchange-correlation potentials rather than giving an accurate exchange–correlation energy. Although the KT functionals cannot compete with the best functionals for thermochemistry, they are very useful for calculation of magnetic properties (for example the NMR shielding constant) which depend—directly and indirectly through the Kohn–Sham orbitals and orbital energies—only on the Kohn–Sham potential, see Refs. [24, 25].

The KT1 functional is

$$E_{\mathrm{XC}}^{\mathrm{KT1}} = E_{\mathrm{XC}}^{\mathrm{LDA}} + \gamma \sum_{\sigma} \int \frac{\left|\nabla \rho_{\sigma}\left(\mathbf{r}\right)\right|^{2}}{\rho_{\sigma}^{4/3}\left(\mathbf{r}\right) + \delta} \, \mathrm{d}\mathbf{r} \tag{1.39}$$

where the parameters γ and δ are introduced and varied to reproduce near exact v_{XC} Zhao–Morrison–Parr (ZMP) potentials [26] constructed from coupled-cluster electron densities (this procedure is described in Section 1.5.5). The γ and δ parameters were then empirically re-fitted to reproduce as accurately as possible, also NMR shielding constants of a set of molecules. The resulting parameters for KT1 are

$$\gamma = -0.006, \delta = 0.1. \tag{1.40}$$

The KT2 functional contains two more parameters $\alpha = 1.07173$ and $\beta = 0.576727$ fitted empirically to improve geometry structures and thermochemical predictions. The

expression is

$$E_{\mathrm{XC}}^{\mathrm{KT2}} = \alpha E_{\mathrm{X}}^{\mathrm{LDA}} + \beta E_{\mathrm{C}}^{\mathrm{LDA}} + \gamma \sum_{\sigma} \int \frac{\left|\nabla \rho_{\sigma}\left(\mathbf{r}\right)\right|^{2}}{\rho_{\sigma}^{4/3}\left(\mathbf{r}\right) + \delta} \, \mathrm{d}\mathbf{r} \tag{1.41}$$

where the γ and δ parameters are those of KT1 Eq.(1.40).

B3LYP

The popular Becke-3-parameter-Lee–Yang–Parr B3LYP functional is an admixture of the LDA, B exchange, LYP correlation and Hartree–Fock exchange energy Eq.(1.35) and it contains three empirical parameters [27]. The inclusion of 20% Hartree–Fock exchange energy makes it a hybrid functional. In the original paper by Becke, the PW91 correlation functional [28] was used in the expression

$$E_{\mathrm{XC}}^{\mathrm{B3PW91}} = E_{\mathrm{XC}}^{\mathrm{LDA}} + a_0 \left(E_{\mathrm{X}}^{\mathrm{HF}} - E_{\mathrm{X}}^{\mathrm{LDA}}\right) + a_{\mathrm{X}} \Delta E_{\mathrm{X}}^{\mathrm{B}} + a_{\mathrm{C}} \Delta E_{\mathrm{C}}^{\mathrm{PW91}} \tag{1.42}$$

The parameters $a_0 = 0.20$, $a_X = 0.72$ and $a_C = 0.81$ were fitted to thermochemical data. Later Stevens *et al.* [29] found a slightly better performance when replacing PW91 with LYP, and the resulting functional is B3LYP.

PBE0

The PBE0 functional [30, 31] is a hybrid functional based on the PBE functional, that contains 25% Hartree–Fock exchange energy,

$$E_{\mathrm{xc}}^{\mathrm{PBE0}} = E_{\mathrm{xc}}^{\mathrm{PBE}} + \frac{1}{4}\left(E_{\mathrm{x}}^{\mathrm{HF}} - E_{\mathrm{x}}^{\mathrm{PBE}}\right). \tag{1.43}$$

It is claimed to contain no empirical parameters as the factor $\frac{1}{4}$ in Eq.(1.43) can be determined from perturbation theory [32].

B97-2 and B97-3

The hybrid B97-2 [33] and B97-3 [34] functionals are based on the B97 functional of Becke [35]. The B97-2 functional contains 21% of Hartree–Fock exchange and is fitted to empirical thermochemical data as well as accurate exchange–correlation potentials determined by wave function electron densities and the ZMP approach. The B97-2 functional contains 10 empirical parameters.

The B97-3 functional is another hybrid functional with 27% exact exchange. It is an extension of the B97-2 functional containing 16 empirical parameters which has been fitted to a larger set of empirical data than B97-2.

CAM-B3LYP

The CAM-B3LYP functional [36] belongs to the class of range separated functionals, meaning that the exchange interaction is described by different mechanisms for short and long interelectron distances. It is possible to write $\frac{1}{r_{12}}$ as

$$\frac{1}{r_{12}} = \frac{[\alpha + \beta \mathrm{erf}\,(\mu r_{12})]}{r_{12}} + \frac{1 - [\alpha + \beta \mathrm{erf}\,(\mu r_{12})]}{r_{12}} \tag{1.44}$$

where α, β and μ are parameters and erf is the error function. The parameterization Eq.(1.44) allow the partitioning of two different exchange energy expressions $E_{\mathrm{X,LR}}$ and $E_{\mathrm{X,SR}}$ both dependent on $\frac{1}{r_{12}}$

$$E_{\mathrm{X}}\,(r_{12}) = E_{\mathrm{X,LR}}\left(\frac{\alpha + \beta \mathrm{erf}\,(\mu r_{12})}{r_{12}}\right) + E_{\mathrm{X,SR}}\left(\frac{1 - [\alpha + \beta \mathrm{erf}\,(\mu r_{12})]}{r_{12}}\right) \tag{1.45}$$

where $E_{\mathrm{X,LR}}$ is the exchange functional whose importance increases at long range and $E_{\mathrm{X,SR}}$ is the exchange functional whose importance increases at short range when α, β and $\alpha + \beta$ take values between 0 and 1. In CAM-B3LYP, the long range $E_{\mathrm{X,LR}}$ is the exact Hartree–Fock exchange energy and the short range $E_{\mathrm{X,SR}}$ is the Becke 1988 functional $E_{\mathrm{X}}^{\mathrm{B}}$. Since the Becke 1988 functional is not explicitly dependent on $\frac{1}{r_{12}}$, it must be re-derived replacing the $\frac{1}{r_{12}}$ operator with $\frac{1-[\alpha+\beta\mathrm{erf}(\mu r_{12})]}{r_{12}}$. A general scheme for this re-derivation of GGA functionals has been developed using the one particle density matrix expressed in the inter-electronic distance r_{12} [36, 37, 38, 39].

The correlation energy in CAM-B3LYP is described by the B3LYP correlation contribution. The fitted parameters are $\alpha = 0.19$, $\beta = 0.46$ and $\mu = 0.33 a_0^{-1}$, with a_0 being the Bohr radius. The sum $\alpha + \beta$ determines the amount of Hartree–Fock exchange at long range which should be equal to 1 for the correct asymptotic behavior of the exchange potential. The performance of CAM-B3LYP for a number of properties was investigated in Paper III.

1.5.4 Optimized Effective Potentials

In the Kohn–Sham operator Eq.(1.30), the effective potential is a multiplicative potential. The functional derivative Eq.(1.32) should therefore be a multiplicative function. However, for orbital-dependent functionals, and in particular the hybrid functionals containing Hartree–Fock exchange, the evaluation of Eq.(1.32) by taking the functional derivative with respect to the electron density directly is not possible. Instead, in conventional applications, the exchange–correlation potential is approximated using

the functional derivative with respect to orbitals using the identity

$$v_{\mathrm{xc}}\phi_i = \frac{\delta E_{\mathrm{xc}}}{\delta \phi_i^*}. \tag{1.46}$$

This approach does however not give a multiplicative potential for functionals that are not locally dependent on the electron density, and is therefore outside the Kohn–Sham scheme.

To come back to the original Kohn–Sham scheme, it is necessary to find the multiplicative potential associated with the orbital-dependent functional. Among all multiplicative potentials, the optimized effective potential (OEP) is the one that minimize the energy when the corresponding orbitals are inserted into the energy expression. The equations to obtain the OEP for Hartree–Fock exchange was first developed by Sharp and Horton [40] after inspiration by Slater [41] and numerical calculations were first performed by Talman and Shadwick on atoms [42].

The OEP may be derived from several starting points, see the review by Engel [43]. We here start by requiring that the OEP minimizes the total energy and therefore the energy is a stationary point with respect to variations in the multiplicative potential when the potential is equal to the OEP

$$\left.\frac{\delta E}{\delta v_{\mathrm{eff}}}\right|_{v_{\mathrm{eff}}=v^{\mathrm{OEP}}} = 0. \tag{1.47}$$

An expression for the functional derivative $\frac{\delta E}{\delta v_{\mathrm{eff}}}$ may be obtained using the chain rule for functional differentiation

$$\frac{\delta E}{\delta v_{\mathrm{eff}}(\mathbf{r})} = \sum_k \left\{ \int \left[\frac{\delta E}{\delta \phi_k^*(\mathbf{r}')} \frac{\delta \phi_k^*(\mathbf{r}')}{\delta v_{\mathrm{eff}}(\mathbf{r})} + \mathrm{c.c.} \right] \mathrm{d}\mathbf{r}' + \frac{\partial E}{\partial \epsilon_k} \frac{\delta \epsilon_k}{\delta v_{\mathrm{eff}}(\mathbf{r})} \right\}, \tag{1.48}$$

where the summation runs over all orbitals and "c.c." denotes the complex conjugate of the preceding term. On the right hand side, all the functional derivatives can be given an explicit expression in terms of v_{eff}, the orbitals and their eigenvalues [43]. Combining these expressions with Eq.(1.47) and Eq.(1.48) results in the following equation

$$\int \chi_{\mathrm{s}}(\mathbf{r},\mathbf{r}')\, v_{\mathrm{xc}}(\mathbf{r}')\, \mathrm{d}\mathbf{r}' = \Lambda_{\mathrm{xc}}(\mathbf{r}), \tag{1.49}$$

where χ_{s} is the Kohn–Sham response function, given by

$$\chi_{\mathrm{s}}(\mathbf{r},\mathbf{r}') = \sum_{ia} \frac{\phi_i^*(\mathbf{r})\,\phi_a(\mathbf{r})\,\phi_a^*(\mathbf{r}')\,\phi_i(\mathbf{r}')}{\epsilon_i - \epsilon_a}, \tag{1.50}$$

which measures the change in the electron density as a result of a change in the effective potential $\frac{\delta \rho}{\delta v_{\mathrm{eff}}}$, and the right hand side of Eq.(1.49) is

$$\Lambda_{\mathrm{xc}}(\mathbf{r}) = \sum_k \left\{ -\int \left[\phi_k^*(\mathbf{r})\, G_k(\mathbf{r},\mathbf{r}') \frac{\delta E_{\mathrm{xc}}}{\delta \phi_k^*(\mathbf{r}')} + \mathrm{c.c.} \right] \mathrm{d}\mathbf{r}' + |\phi_k(\mathbf{r})|^2 \frac{\partial E_{\mathrm{xc}}}{\partial \epsilon_k} \right\}, \tag{1.51}$$

where the G_k are Green's functions

$$G_k(\mathbf{r},\mathbf{r}') = \sum_{l\neq k} \frac{\phi_l(\mathbf{r})\,\phi_l^*(\mathbf{r}')}{\epsilon_l - \epsilon_k}. \tag{1.52}$$

The solution of Eq.(1.49)—the potential v_{xc}— is the optimized effective exchange–correlation potential of the energy functional for a given a set of orbitals and orbital energies.

We continue, restricting the non-local orbital-dependent functional to be the exact-exchange functional Eq.(1.35). The stable solution of the integral equations Eq.(1.49) is difficult due to often-encountered singularities in the Kohn–Sham response function. Because of this, several approximations have been developed to find the OEP, see for example the recent review of Kümmel and Kronik [44]. The approach used for calculations in this thesis is that of Yang and Wu [45, 46], where the effective multiplicative potential to be used in the Kohn–Sham operator Eq.(1.30) is written

$$v_{\text{eff}}(\mathbf{r}) = v_{\text{nuc}}(\mathbf{r}) + v_{\text{ref}}(\mathbf{r}) + \sum_t b_t g_t(\mathbf{r}). \tag{1.53}$$

Here v_{nuc} is the nuclear attraction potential, and v_{ref} is a fixed reference potential for example constructed from a Hartree–Fock-optimized electron density in the Fermi–Amaldi potential [47]

$$v_{\text{ref}} = \frac{N-\xi}{N}\int \frac{\rho(\mathbf{r})\,\rho(\mathbf{r}')}{|\mathbf{r}-\mathbf{r}'|}\,\mathrm{d}\mathbf{r}'. \tag{1.54}$$

where ξ is the fraction of Hartree–Fock exchange in the functional (e.g. $\xi = a_0 = 0.2$ for the B3LYP functional Eq.(1.42)). The purpose of v_{ref} is to account for a large proportion of the electron–electron interaction part of v_{eff}, and also to ensure the correct long range behavior of the effective potential. The third term in Eq.(1.53) is an expansion in an auxiliary basis set g_t with expansion coefficients b_t. In the Yang–Wu OEP scheme, since the only parameters in the potential Eq.(1.53) that may vary are the b_t coefficients, the functional derivative of the stationary condition Eq.(1.47) can be written

$$\frac{\delta E}{\delta v_{\text{eff}}} = \frac{\partial E}{\partial b_t} = \sum_i \int \left[\frac{\delta E}{\delta \phi_i^*(\mathbf{r}')}\frac{\delta \phi_i^*(\mathbf{r}')}{\delta v_{\text{eff}}(\mathbf{r})}\frac{\partial v_{\text{eff}}}{\partial b_t} + \text{c.c.}\right]\mathrm{d}\mathbf{r}'. \tag{1.55}$$

The sum is over the occupied orbitals i and the term corresponding to the last term of Eq.(1.48) does not appear in Eq.(1.55) since $\frac{\partial E}{\partial \epsilon_k} = 0$ when the non-local functional form consists of Hartree–Fock exchange. Evaluating the terms in Eq.(1.55) yields [45]

$$\frac{\partial E}{\partial b_t} = \sum_{ia} \int \left[\frac{\delta E}{\delta \phi_i^*(\mathbf{r}')}\phi_a(\mathbf{r})\frac{<\phi_a|g_t|\phi_i>}{\epsilon_i - \epsilon_a} + \text{c.c.}\right]\mathrm{d}\mathbf{r} \tag{1.56}$$

where a runs over the virtual orbitals. The optimization of the b_t coefficients may now be performed by iterative techniques exploiting the derivative energy expression and the stationary condition Eq.(1.47). When the auxiliary functions g_t in Eq.(1.53) are chosen to be Gaussian functions, the calculation of the gradient Eq.(1.56) requires the evaluation of three-center overlap integrals over Gaussian basis functions in $< \phi_a | g_t | \phi_i >$.

For a practical OEP calculation, the computational strategy can be as follows:

1. Input a set of trial orbitals and orbital eigenvalues $\{\phi_k, \epsilon_k\}$
2. Construct the OEP determining equations from the input orbitals and orbital eigenvalues
3. Solve the OEP equations iteratively to find the OEP
4. Using the the OEP, solve the Kohn–Sham equations to yield new orbitals and orbital energies
5. Iterate from 2 till the orbitals do not change from last iteration (the orbitals are self consistent)

The OEP Kohn–Sham calculation is therefore more involved than the regular SCF optimization of the Kohn–Sham orbitals (similar to the procedure described for Hartree–Fock theory in Section 1.4.2), requiring also the iterative solution of the OEP potential in each SCF iteration in step 3.

1.5.5 Density-Corresponding Potentials

We define here the density-corresponding potential (DCP) as the solution to the following problem: Given an electron density, find the corresponding Kohn–Sham effective potential (the DCP), orbitals and eigenvalues. In this thesis, the motivation for using DCPs is to obtain accurate exchange–correlation potentials from accurate coupled-cluster electron densities, and then to use the resulting DCP for calculations of magnetic properties.

Several schemes have been developed to find the DCP, see the references in [48]. Some solutions to the DCP problem, including the Zhao–Morrison–Parr (ZMP) [26] and the Wu–Yang (WY) methods [48], are based on the Levy constrained-search functional [7]. The Levy constrained-search functional,

$$Q\left[\rho\right] = \min_{\Psi_\rho} < \Psi_\rho | \hat{T} + \hat{V}_{ee} | \Psi_\rho >, \tag{1.57}$$

minimizes the sum of the kinetic and electron–electron repulsion energies, searching over all antisymmetric wave functions Ψ_ρ that yield a density ρ. The functional Q is in fact a generalization of the Hohenberg–Kohn functional F of Eq.(1.22) where, for Q, the constraints on ρ are less severe. The requirement in the Hohenberg–Kohn functional that ρ is v-representable is replaced in Eq.(1.57) with the requirement that ρ is N-representable—that is, ρ is obtained from an antisymmetric wave function.

The Kohn–Sham orbitals corresponding to an electron density can be found by minimizing the noninteracting kinetic energy [49]

$$T_{\mathrm{s}} = \min_{\Phi \to \rho} < \Phi | \hat{T} | \Phi > \tag{1.58}$$

under the constraint that the electron density is given by the sum of squares of the occupied orthonormal orbitals, Eq.(1.24). In Eq.(1.58), Φ is the Kohn–Sham determinant, and the right hand side corresponds to the Levy constrained-search functional Eq.(1.57) without $\hat{V}_{ee}$ (this term is constant for a fixed density assuming that the electron–electron interaction depends locally on the electron density). In a constrained optimization of the orbitals determining the minimum T_{s}, using the method of Lagrange multipliers for the constraints $\rho = \sum_i \phi_i^* \phi_i$ and $< \phi_i | \phi_j >= \delta_{ij}$, the Kohn–Sham equations are recovered where the Lagrange multiplier for the density appears as the effective Kohn–Sham potential and the multipliers for the orthonormality of the orbitals appear as orbital energies [7]. The effective potential that yields the desired electron density must then be searched for in some manner. Assuming this effective potential (the DCP) is found, the corresponding exchange–correlation potential can be obtained by subtracting the nuclear-attraction and Coulomb-repulsion potentials from the DCP.

In this thesis, the WY-scheme [48] has been applied to obtain DCPs. Here, the effective potential is written in the form of Eq.(1.53) and varied to minimize the kinetic energy under the constraint that the electron density is equal to the input electron density. For the constrained minimization, the Lagrangian function

$$W_{\mathrm{s}} \left[\Phi, v \left(\mathbf{r} \right) \right] = \sum_i < \phi_i | \hat{T} | \phi_i > + \int v \left(\mathbf{r} \right) \left(\rho \left(\mathbf{r} \right) - \rho_{\mathrm{inp}} \left(\mathbf{r} \right) \right) \mathrm{d}\mathbf{r} \tag{1.59}$$

is set up, where $v \left(\mathbf{r} \right)$ is a Lagrange multiplier for the constraint that the electron density ρ is equal to the input electron density ρ_{inp}. It can be shown that the non-interacting kinetic energy is found by a combined minimization and maximization of Eq.(1.59) [48]

$$T_{\mathrm{s}} \left[\rho_{\mathrm{inp}} \right] = \max_{v(\mathbf{r})} \left\{ \min_{\phi_i, < \phi_i | \phi_i > = 1} W_{\mathrm{s}} \left[\Phi, v \left(\mathbf{r} \right) \right] \right\} \tag{1.60}$$

Using the potential form Eq.(1.53), the determination of $T_{\mathrm{s}} \left[\rho_{\mathrm{inp}} \right]$ turns into an unconstrained maximization of W_{s} with respect to the expansion coefficients b_t. The

maximization can be performed when the derivatives of W_s with respect to the b_t are known. Analytical expressions for the derivatives are given in Ref. [48]. Once the coefficients b_t are known, the DCP is given by Eq.(1.53).

1.5.6 Current-Density-Functional Theory

In the presence of a magnetic field, the original Hohenberg–Kohn theorems are no longer valid. This is due to the fact that the electron density only determines the external scalar potential, and not the external vector potential associated with the magnetic field. There is consequently no longer a unique mapping between the electron density and the external potentials. As a result, the Hamiltonian and wave function can no longer be determined by the electron density alone.

The Hohenberg–Kohn theorems may be generalized to be valid also in the presence of a magnetic field by extending the theory to also consider the electron current-density. That is, together the ground-state electron density and current-density determines the scalar and vector potentials uniquely. This formalism, where the exchange–correlation energy functional is a functional of both the electron current-density and the electron density is named current-density-functional theory (CDFT).

Clearly, to calculate the response of an electronic system to a perturbing magnetic field in a formally correct manner, it is necessary to work within CDFT. Nevertheless, most DFT calculations on magnetic properties in the literature are performed using the regular DFT functionals, effectively setting the current dependence of the exchange–correlation energy to zero. It is widely believed that the current-density dependence of the exchange–correlation functional has a very small effect on the computed values. This is mainly based on the calculations of Handy and co-workers [50, 51, 52], where the Vignale–Rasolt–Geldart (VRG) current-density functional [12, 53] was used (added to a regular DFT functional) to calculate magnetizabilities and NMR shielding constants. The error in the regular density functional was found to swamp the effect of adding the current-dependent VRG contribution, and also disappointingly, the current contribution shifted the results further away from experimental values. These studies have discouraged the use of the more complicated CDFT for calculations of magnetic properties. Indeed, practitioners of DFT magnetic property calculations are often stating in the literature that the current dependence is small and therefore does not need consideration. In this thesis, CDFT has not been used, but observations have been made indicating that the CDFT contributions should be reconsidered, see Paper VIII and Ch. 5.

Chapter 2

Benchmark of DFT Methods

When an approximate theory is used to predict values for molecular properties, it is important to know the expected accuracy of the result. Without this knowledge, it is impossible to establish to what degree the result of the calculation can be trusted, thereby rendering the calculation meaningless. For DFT methods, which lack a procedure for systematic improvement towards an exact solution of the electronic problem, measures of the expected accuracy can only be achieved by performing benchmark studies where the results of the DFT methods are tested against accurate benchmark data. It is important to carefully consider also the quality of the benchmark data — the benchmark data should not contain errors so large that the error measures of the tested functional is affected significantly. This would lead to false conclusions and misunderstanding, hampering the development of new and better density functionals.

In this Chapter, some general considerations when testing the performance of DFT methods are presented. We begin by discussing the discrepancy between the exact electronic solution within the Born–Oppenheimer approximation and experimentally measured values in Section 2.1. Next, in Section 2.2, the discussion considers the discrepancies between the exact electronic solution and practical DFT calculations of properties. Finally, in Section 2.3, a general discussion of the choice of benchmark data for testing DFT methods is given.

2.1 The Experiment and the Exact Electronic Solution

Experimental measurements of molecular properties are performed under widely various conditions. For example, the experiment may be performed in solid, liquid or

Figure 2.1: The sources of discrepancy between experimental measurement, the exact electronic solution within the Born–Oppenheimer approximation and a practical DFT calculation.

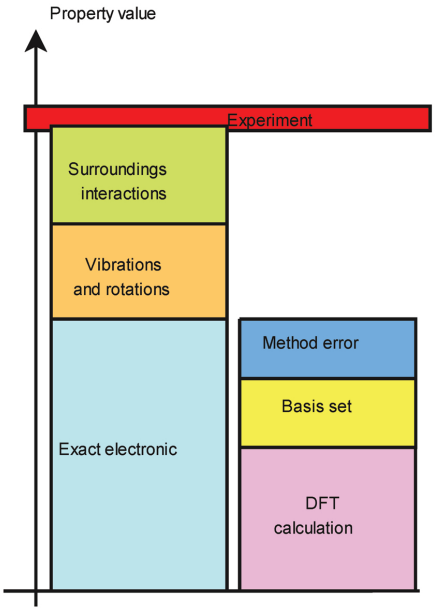

gas phase. Also, depending on the experimental situation, the molecule under study will be surrounded by solvent molecules which in various ways affect the result of the measurement. In addition, the measurement will depend on the thermodynamic variables such as temperature, since the population of states varies with these variables. In summary, we may say that experimental measurements are affected by solvation and temperature effects.

When performing a calculation with an exact model on a single molecule within the Born–Oppenheimer approximation, we obtain the exact result for a non-vibrating, non-rotating molecule unaffected by surroundings. Clearly, the calculation will not give the same result as experiment — there is a discrepancy between theory and experiment due to solvation, vibrations and rotations and also possibly experimental errors.

The situation is illustrated in Figure 2.1, where the red top line represents the experimental value for the property and the thickness of the line represents the experimental uncertainty. On the left of the figure, the result of a calculation using the exact theory within the Born–Oppenheimer approximation is represented by the blue box. The discrepancy between experiment and theory is separated into two contributions, those arising from nuclear motions and those arising from effects caused by the surroundings.

2.2 Approximate Calculations and the Exact Electronic Solution

In a practical calculation, using for example DFT, there are additional sources of error between theory and experiment, related to the incomplete description of the electronic system. First, when using a limited basis set to expand the one-electron functions Eq.(1.9), the incompleteness of the basis set give source to the basis-set error, represented by the yellow box in Fig. 2.1. The size of the basis-set error can be estimated by investigating the convergence of the property with systematic extension of the basis set.

Secondly, the intrinsic error of the method, represented by the blue box in Fig. 2.1, is, in DFT, due to the inaccurate form of the exchange–correlation functional, or for a wave-function method, the truncation of the many-electron space Eq.(1.16). For wave-function methods, it is possible to estimate the size of the intrinsic error by studying the convergence of the properties when systematically increasing the number of determinants in the wave function (i.e. increasing the excitation level in the truncated

cluster operator for CC methods) . For DFT methods, this approach is not possible and testing against high quality benchmark data is necessary to obtain information about the intrinsic error.

Part of the intrinsic method error may be due to a non-relativistic treatment of the electronic structure problem, the so called relativistic effects. Relativistic effects are generally small for first and second row atoms and we do not study molecules containing heavier nuclei here.

It is worth noting that for a practical calculation, the different sources of error found in Figure 2.1 may have opposite signs, thereby fortuitously canceling each other. A well known example is the good results obtained by Hartree–Fock theory in connection with a small double-zeta basis set, where the basis-set error and the method error often cancel very well.

2.3 Benchmark values

To be able to test DFT methods in the ability to predict some property, a set of assumed correct benchmark values must be chosen for comparison. There are two main sources of benchmark values: Experimental measurements and accurate wave function results. There are problems with both choices which will be discussed below.

Let us first point out that the aim of a DFT calculation must be to reproduce as accurately as possible the result of the exact electronic solution. Therefore, the direct comparison with experimental data is only appropriate when the experimental error bars are not too large and when the ro-vibrational and solvation effects are small or corrected for, see Figure 2.1. If these errors are large, the benchmark values will be of low quality, leading to error measures of the tested functionals that are inaccurate or even misleading, as the real intrinsic DFT errors are disguised by large errors in the benchmark data.

So, to be able to compare results with experiment, ro-vibrational and solvation effects should be accounted for. These effects may in some cases be measured or estimated in experiment, however, in general they are not known and must be modeled by calculations. These calculations are usually expensive, and also in many cases difficult to treat accurately.

With the aforementioned difficulties of using experimental values for the benchmark data in mind, it may seem better to use accurate wave function methods to produce benchmark values. In this case, the problems related to solvation, rotations and vibra-

tions are removed as both the DFT methods and the wave function methods can be performed within the Born–Oppenheimer approximation on single isolated molecules. It is then possible to calculate the property at a single nuclear geometry, comparing the results directly. There are, however, also difficulties using this approach. The accuracy of the wave function method used should be estimated by studying the convergence of the property with regard to the correlation treatment and the one-electron basis. For well converged results, at least the CCSD(T) method should be used and in some cases even better wave functions must be employed. The cost of these calculations are large, and benchmark data can only be obtained for small molecules. This highlights one of the advantages of using experimental data, which can be obtained for a wider range of both large and small molecules.

Chapter 3

Molecular Properties

In this Chapter, the molecular magnetic properties studied in this thesis will be introduced. The properties are identified as derivatives of the energy in Section 3.1. Then, the theory for the calculation of magnetic properties is described, setting up the Hamiltonian in the presence of magnetic fields in Section 3.2, describing the gauge-origin dependence problem in Section 3.3 and finding analytical energy derivative expressions in Section 3.4 using linear response theory in Section 3.5. The expressions for the energy derivatives are also described by perturbation theory in Section 3.6. The magnetic properties are finally given a qualitative description in Section 3.7.

3.1 Identification of Spectroscopic Constants

Many spectroscopic constants can, in the static case, be identified as energy derivatives with respect to perturbing magnetic or electric fields. To see this, we first write the energy as a Taylor expansion in a perturbing field $\mathbf{F}$

$$E(\mathbf{F}) = E_0 + \frac{\mathrm{d}E}{\mathrm{d}\mathbf{F}}\mathbf{F}\bigg|_{\mathbf{F}=0} + \frac{1}{2}\,\mathbf{F}^{\mathrm{T}}\frac{\mathrm{d}^2E}{\mathrm{d}\mathbf{F}\mathrm{d}\mathbf{F}}\mathbf{F}\bigg|_{\mathbf{F}=0} + \ldots \tag{3.1}$$

Here, E_0 is the energy in the absence of a perturbing field, and all the derivatives are taken at zero perturbing field.

Although $\mathbf{F}$ may represent any perturbation, the interests in this work are different perturbing magnetic fields, in particular, an external homogeneous magnetic field $\mathbf{B}$, the magnetic field $\mathbf{M}_K$ associated with the spin of a nucleus $\mathbf{I}_K$ and its gyromagnetic ratio γ_K

$$\mathbf{M}_K = \gamma_K \mathbf{I}_K \tag{3.2}$$

and also, the magnetic like perturbation associated with the total angular momentum $\mathbf{J}$ of a rotating molecule. We may collect all these perturbations into a vector

$$\mathbf{F} = \{\mathbf{B}, \mathbf{M}_K, \mathbf{J}\} \tag{3.3}$$

Comparing the expression Eq.(3.1) (where $\mathbf{F}$ is replaced according to Eq.(3.3)), with effective Hamiltonian expressions in the presence of $\mathbf{B}$, $\mathbf{M}_K$ and $\mathbf{J}$ perturbations where the electron behavior appears as parameters [54, 55, 56] (including only second-order terms since the first-order terms vanish for closed shell molecules)

$$\begin{aligned} H_{\text{eff}} &= -\sum_K \mathbf{B}^{\mathrm{T}} \left(1 - \boldsymbol{\sigma}_K\right) \mathbf{M}_K + \frac{1}{2} \sum_{K \neq L} \mathbf{M}_K^{\mathrm{T}} \left(\mathbf{D}_{KL} + \mathbf{K}_{KL}\right) \mathbf{M}_L \\ &\quad + \frac{1}{2} \mathbf{J}^{\mathrm{T}} \mathbf{I}_{\text{eff}}^{-1} \mathbf{J} - \mu_{\text{n}} \mathbf{J}^{\mathrm{T}} \mathbf{g} \mathbf{B} - \frac{1}{2} \mathbf{B}^{\mathrm{T}} \boldsymbol{\xi} \mathbf{B} - \mathbf{J}^{\mathrm{T}} \mathbf{C}_K \mathbf{M}_K, \end{aligned} \tag{3.4}$$

it is possible to identify and define the following tensors

$$\mathbf{g} = -\frac{1}{\mu_{\text{n}}} \left. \frac{\mathrm{d}^2 E}{\mathrm{d}\mathbf{J}\mathrm{d}\mathbf{B}} \right|_{\mathbf{J},\mathbf{B}=0} \tag{3.5}$$

$$\boldsymbol{\xi} = -\left. \frac{\mathrm{d}^2 E}{\mathrm{d}\mathbf{B}\mathrm{d}\mathbf{B}} \right|_{\mathbf{B}=0} \tag{3.6}$$

$$\mathbf{C}_K = -\left. \frac{\mathrm{d}^2 E}{\mathrm{d}\mathbf{J}\mathrm{d}\mathbf{M}_K} \right|_{\mathbf{J},\mathbf{M}_K=0} \tag{3.7}$$

$$\boldsymbol{\sigma}_K = \left. \frac{\mathrm{d}^2 E}{\mathrm{d}\mathbf{B}\mathrm{d}\mathbf{M}_K} \right|_{\mathbf{B},\mathbf{M}_K=0} + \mathbf{1} \tag{3.8}$$

$$\mathbf{K}_{KL} = \left. \frac{\mathrm{d}^2 E}{\mathrm{d}\mathbf{M}_K\mathrm{d}\mathbf{M}_L} \right|_{\mathbf{M}_K,\mathbf{M}_L=0} - \mathbf{D}_{KL} \tag{3.9}$$

where the three-by-three tensors are the rotational g-tensor $\mathbf{g}$, the magnetizability tensor $\boldsymbol{\xi}$, the spin-rotation tensor $\mathbf{C}_K$, the nuclear shielding tensor $\boldsymbol{\sigma}_K$ and the reduced indirect nuclear spin–spin coupling tensor $\mathbf{K}_{KL}$. Note that the sign of the spin-rotation constant used here is opposite of the sign convention of Flygare [56] but the same convention as used by experimentalists. In Eq.(3.4), the tensor $\mathbf{D}_{KL}$ represents the direct coupling of the magnetic dipole moments of the nuclei, $\mathbf{I}_{\text{eff}}$ is the moment of inertia tensor of the molecule and μ_{n} is the nuclear magneton.

3.2 The Hamiltonian and the Energy in Magnetic Fields

Having identified the second-order magnetic properties in Section 3.1 in terms of energy derivatives Eq.(3.5) – (3.9), we proceed to the calculation of such derivatives. The first

step in finding expressions for the energy derivatives is to find the expression for the energy itself. The energy is determined by the form of the Hamiltonian operator.

When a rotating molecule is placed in a magnetic field and is under influence of the magnetic dipole moments of the nuclei, the Hamiltonian operator Eq.(1.3) must include new energy terms arising from the interactions of the magnetic fields and the moving charged particles. This analysis must also include the interaction of the magnetic fields with the magnetic moments of the electrons $\mathbf{m}_i$,

$$\mathbf{m}_i = -\mathbf{s}_i \tag{3.10}$$

where $\mathbf{s}_i$ is the spin of the electron.

To allow for the rotation of the nuclei in the molecule implies a partial lifting of the Born–Oppenheimer approximation Eq.(1.3). Here we only allow the nuclear framework to rotate rigidly and neglect nuclear vibrations. The nucleus–nucleus repulsion of the full Hamiltonian Eq.(1.2) is then a constant and the kinetic energy operator of the nuclei is constrained to the kinetic energy operator of rigid rotations of the nuclear framework. A presentation of the derivation of the Hamiltonian for a rotating molecule in the presence of an external magnetic field and nuclear magnetic moments has been given by Flygare [56]. The terms arising from nuclear spin–spin interactions is for instance discussed by Ramsey [57] and McWeeny [58]. The Hamiltonian is

$$\begin{aligned}
H &= H_0 && (3.11)\\
&\quad + \frac{1}{2}\mathbf{B}\cdot\mathbf{L}_{\mathrm{O}} + \frac{1}{8}\mathbf{B}^{\mathrm{T}}\left(\sum_i r_{i\mathrm{O}}^2\mathbf{I}_3 - \mathbf{r}_{i\mathrm{O}}\mathbf{r}_{i\mathrm{O}}^{\mathrm{T}}\right)\mathbf{B} && (3.12)\\
&\quad + \alpha^2\sum_K \mathbf{M}_K\cdot\sum_i \frac{\mathbf{l}_{iK}}{r_{iK}^3} + \frac{\alpha^4}{2}\sum_K\sum_{L\neq K}\mathbf{M}_K^{\mathrm{T}}\sum_i \frac{\left(\mathbf{r}_{iK}\mathbf{r}_{iL}^{\mathrm{T}}\right)\mathbf{I}_3 - \mathbf{r}_{iK}\mathbf{r}_{iL}^{\mathrm{T}}}{r_{iK}^3 r_{iL}^3}\mathbf{M}_L && (3.13)\\
&\quad + \frac{\alpha^2}{2}\sum_K \mathbf{M}_K^{\mathrm{T}}\sum_i\left(\frac{\left(\mathbf{r}_{i\mathrm{O}}\cdot\mathbf{r}_{iK}\right)\mathbf{I}_3 - \mathbf{r}_{iK}\mathbf{r}_{i\mathrm{O}}^{\mathrm{T}}}{r_{iK}^3}\right)\mathbf{B} && (3.14)\\
&\quad + \frac{1}{2}\mathbf{J}^{\mathrm{T}}\mathbf{I}_{\mathrm{n}}^{-1}\mathbf{J} - \mathbf{J}^{\mathrm{T}}\mathbf{I}_{\mathrm{n}}^{-1}\mathbf{L}_{\mathrm{CM}} + \frac{1}{2}\mathbf{L}_{\mathrm{CM}}^{\mathrm{T}}\mathbf{I}_{\mathrm{n}}^{-1}\mathbf{L}_{\mathrm{CM}} && (3.15)\\
&\quad - \frac{1}{2}\mathbf{B}^{\mathrm{T}}\sum_K\left(Z_K r_{K,\mathrm{CM}}^2\mathbf{I}_3 - \mathbf{r}_{K,\mathrm{CM}}\mathbf{r}_{K,\mathrm{CM}}^{\mathrm{T}}\right)\mathbf{I}_{\mathrm{n}}^{-1}\left(\mathbf{J}-\mathbf{L}_{\mathrm{CM}}\right) && (3.16)\\
&\quad + \frac{1}{8}\mathbf{B}^{\mathrm{T}}\sum_K\frac{Z_K^2}{M_K}\left(r_{K,\mathrm{CM}}^2\mathbf{I}_3 - \mathbf{r}_{K,\mathrm{CM}}\mathbf{r}_{K,\mathrm{CM}}^{\mathrm{T}}\right)\mathbf{B} && (3.17)\\
&\quad - \frac{\alpha^2}{2}\sum_K\sum_{L\neq K}\mathbf{M}_K^{\mathrm{T}}\frac{Z_L}{r_{KL}^3}\left(r_{KL}^2\mathbf{I}_3 - \mathbf{r}_{KL}\mathbf{r}_{KL}^{\mathrm{T}}\right)\mathbf{I}_{\mathrm{n}}^{-1}\left(\mathbf{J}-\mathbf{L}_{\mathrm{CM}}\right) && (3.18)\\
&\quad - \sum_K \mathbf{M}_K\cdot\mathbf{B} + \sum_i \mathbf{m}_i\cdot\mathbf{B} && (3.19)
\end{aligned}$$

$$+\sum_i \mathbf{m}_i^{\mathrm{T}} \left[\sum_K \left(-\alpha^2 \frac{r_{iK}^2 \mathbf{I}_3 - 3\mathbf{r}_{iK}\mathbf{r}_{iK}^{\mathrm{T}}}{r_{iK}^5} + \frac{8\pi\alpha^2}{3}\delta\left(\mathbf{r}_{iK}\right)\mathbf{I}_3 \right) \mathbf{M}_K \right] \tag{3.20}$$

$$+\frac{1}{2}\sum_K \sum_{L\neq K} \mathbf{M}_K^{\mathrm{T}} \frac{r_{KL}^2 \mathbf{I}_3 - 3\mathbf{r}_{KL}\mathbf{r}_{KL}^{\mathrm{T}}}{r_{KL}^5} \mathbf{M}_L. \tag{3.21}$$

H_0 is the Hamiltonian of a non-rotating molecule in the absence of magnetic fields Eq.(1.3) and $\mathbf{I}_3$ is the three-by-three identity matrix. The terms in Eq.(3.12)–(3.14) originate from the introduction of the generalized momentum operator for the electrons

$$\boldsymbol{\pi}_i = -\mathrm{i}\nabla_i + \mathbf{A} \tag{3.22}$$

which must replace the momentum operators of Eq.(1.2) when the particles move in a magnetic field represented by the vector potential $\mathbf{A}$. Here $\mathbf{A}$ is the vector potential associated with the external magnetic field and the nuclear magnetic moments

$$\mathbf{A} = \mathbf{A}^{\mathrm{ext}} + \mathbf{A}^{\mathrm{nuc}} \tag{3.23}$$

$$\mathbf{A}^{\mathrm{ext}} = \frac{1}{2}\left(\mathbf{B}\times\mathbf{r}_{i\mathrm{O}}\right), \quad \mathbf{A}^{\mathrm{nuc}} = \sum_K \alpha^2 \frac{\mathbf{M}_K \times \mathbf{r}_{iK}}{r_{iK}^3}. \tag{3.24}$$

In Eq.(3.24), α is the fine structure constant and $\mathbf{r}_{i\mathrm{O}}$ is the distance vector between the point $\mathbf{r}_i$ and the physically arbitrary chosen gauge origin $\mathbf{O}$ of the vector potential. Gauge origins are discussed in more detail in Section 3.3. Further, in Eq.(3.12), the total electronic orbital angular momentum is

$$\mathbf{L}_{\mathrm{O}} = \sum_i \mathbf{l}_{i\mathrm{O}} = -\mathrm{i}\sum_i \mathbf{r}_{i\mathrm{O}} \times \nabla_i \tag{3.25}$$

where i runs over all electrons. In Eq.(3.12) are the terms giving rise to the paramagnetic and diamagnetic magnetizability, respectively. Similarly, in Eq.(3.13) are the terms that give rise to the paramagnetic spin–orbit and diamagnetic spin–orbit contributions to the indirect NMR spin–spin coupling constants. The term in Eq.(3.14) is responsible for the diamagnetic contribution to the NMR shielding constant.

Further, in Eq.(3.15) are extra terms to the kinetic energy from the rotational movement of the molecule. In Eq.(3.15), $\mathbf{I}_{\mathrm{n}}^{-1}$ is the inverse of the nuclear moment of inertia in the principal axis system. CM denotes the center of mass. The second term of Eq.(3.15) gives contributions to the rotational g-tensor and the spin–rotation constants as a result of the non-Born–Oppenheimer coupling of nuclear and electronic motion.

In Eq.(3.16) and Eq.(3.17) are terms arising from the generalized momentum treatment of the rotating nuclei, and Eq.(3.18) is a sum of terms describing the interaction

of the magnetic moment of a nucleus with the the magnetic field generated by the other moving nuclei due to the molecular rotation. These terms, Eq.(3.16)–(3.18), give rise to the nuclear contributions to the rotational g-tensor, magnetizability and spin–rotation constants, respectively.

Next are the terms in Eq.(3.19) describing the interactions between the external magnetic field and the magnetic moments of the nuclei and the electrons. In Eq.(3.20) are terms from the interactions of the magnetic dipoles of the nuclei with the magnetic dipoles of the electrons. The content of the square brackets is the magnetic field from nuclei, obtained by taking $\mathbf{B}^{\text{nuc}} = \nabla \times \mathbf{A}^{\text{nuc}}$, and contains a dipole–dipole interaction term and a contact term giving rise to the spin–dipolar and Fermi–contact contributions to the indirect NMR spin–spin coupling constants.

Finally, in Eq.(3.21) are the direct magnetic dipole–dipole interactions of the nuclei. In liquid and gas phase measurements, these couplings vanish due to the rotation of the molecule.

3.3 Gauge-Origin Dependence

A homogeneous magnetic field $\mathbf{B}$ may be represented by the vector potential

$$\mathbf{A}_{\text{O}} = \frac{1}{2}\mathbf{B} \times (\mathbf{r} - \mathbf{r}_{\text{O}}) \,. \tag{3.26}$$

as already noted in Eq.(3.24), where $\mathbf{r}_{\text{O}}$ is the position of the gauge origin, the point where the vector potential vanish. The position of the gauge origin is physically arbitrary as it corresponds to a gauge transformation of the vector potential. In quantum chemical calculations using a finite conventional basis set however, the result of a calculation is dependent on the gauge origin [59]. This unphysical behavior is undesirable and is known as the gauge-origin problem. As a byproduct of the gauge-origin problem, large basis sets must be employed to obtain converged results for magnetic field perturbations.

Several schemes has been proposed to handle the gauge-origin problem, see the discussion in Ref. [55]. The most robust method has shown to be gauge-invariant atomic orbitals (GIAO's) or London atomic orbitals,ω_α , first used by London [60] (and later in an efficient analytical derivative implementation by Wolinski, Hinton and Pulay [61]) where the regular basis functions Eq.(1.10) are equipped with complex phase factors containing the magnetic field

$$\omega_\alpha(\mathbf{B}) = \exp\left[-\mathrm{i}\mathbf{A}_\alpha^{\mathbf{B}} \cdot \mathbf{r}\right] \chi_\alpha \tag{3.27}$$

where

$$\mathbf{A}_{\alpha}^{\mathbf{B}} = \frac{1}{2}\mathbf{B} \times (\mathbf{R}_{\alpha} - \mathbf{r}_{\mathrm{O}}), \tag{3.28}$$

and $\mathbf{R}_{\alpha}$ is the distance vector to the nuclear center where the basis function is centered. The London atomic orbitals ensure that for atomic systems, the unperturbed wave function is an eigenfunction of the perturbed Hamiltonian to first order in the magnetic field [55]. In addition to give results for molecular properties independent of the choice of gauge origin, the basis-set convergence is also much faster with the London atomic orbitals.

Taking advantage of the similarity of the magnetic field perturbation and the perturbation of rotational motion, Gauss, Ruud and Helgaker [62] proposed the *rotational* London atomic orbitals

$$\omega_{\alpha}(\mathbf{B}, \mathbf{J}) = \exp\left[-\mathrm{i}\left(\mathbf{A}_{\alpha}^{\mathbf{B}} + \mathbf{A}_{\alpha}^{\mathbf{J}}\right) \cdot \mathbf{r}\right] \chi_{\alpha} \tag{3.29}$$

to improve also the basis-set convergence in the calculation of spin-rotation constants and rotational g-tensors. The additional term in the phase factor is

$$\mathbf{A}_{\alpha}^{\mathbf{J}} = -\mathbf{I}^{-1}\mathbf{J} \times \mathbf{R}_{\alpha} \tag{3.30}$$

and $\mathbf{I}^{-1}$ is the inverse of the moment of inertia tensor. All calculations in this work are done using (rotational) London atomic orbitals.

The inclusion of the rotational London atomic orbital phase factor in the basis functions makes the basis functions dependent on $\mathbf{B}$ and $\mathbf{J}$ and therefore dependent on these perturbations. This means that molecular orbitals constructed from rotational London atomic orbitals do not automatically stay orthonormal when the magnetic field or the rotational angular momentum change. To preserve orthonormality, we may introduce a connection matrix $\mathbf{T}$ such that [63, 64]

$$\phi_{i}^{\mathrm{OMO}}(\mathbf{B}, \mathbf{J}) = \sum_{r} \mathbf{T}(\mathbf{B}, \mathbf{J})_{ir}\, \phi_{r}^{\mathrm{UMO}}(\mathbf{B}, \mathbf{J}) \tag{3.31}$$

where the unorthonormal orbitals $\phi_{r}^{\mathrm{UMO}}(\mathbf{B}, \mathbf{J})$ are constructed in the regular manner as in Eq.(1.9) and the orbitals $\phi_{i}^{\mathrm{OMO}}(\mathbf{B}, \mathbf{J})$ are orthonormal for any $\mathbf{B}$ or $\mathbf{J}$. The connection matrix should satisfy the equation

$$\mathbf{T}^{\mathrm{T}}(\mathbf{B}, \mathbf{J})\, \mathbf{S}(\mathbf{B}, \mathbf{J})\, \mathbf{T}(\mathbf{B}, \mathbf{J}) = \mathbf{1} \tag{3.32}$$

where $\mathbf{S}$ is the overlap matrix. Eq.(3.32) can easily be seen to hold for $\mathbf{T} = \mathbf{S}^{-1/2}$, however any $\mathbf{T}$ that fulfills Eq.(3.32) can be used. A numerically more stable $\mathbf{T}$, the *natural* connection, has been discussed by Olsen *et al.* [65].

3.4 Energy Derivatives

We follow here closely the exposition of Helgaker *et al.* [55]. To evaluate the energy derivatives in Eq.(3.5)–(3.9), we start by writing the energy as a function of the variational parameters and the perturbing fields

$$E = E\left(\boldsymbol{\lambda}, \mathbf{F}\right) \tag{3.33}$$

where $\boldsymbol{\lambda}$ are the variational parameters and $\mathbf{F}$ represent the perturbing fields Eq.(3.3). The variational parameters $\boldsymbol{\lambda}$ are dependent on the external field, and for each field strength, there is a set $\boldsymbol{\lambda}_0$ giving the lowest energy such that

$$E_0 = E\left(\boldsymbol{\lambda}, \mathbf{F}\right)|_{\boldsymbol{\lambda}=\boldsymbol{\lambda}_0} \tag{3.34}$$

fulfilling the variational condition Eq.(1.8) for all field strengths.

In the next, we assume that the energy derivatives are taken at zero perturbation, $\mathbf{F} = 0$. The first derivative of the energy with respect to the external field is

$$\frac{\mathrm{d}E_0}{\mathrm{d}\mathbf{F}} = \frac{\partial E_0}{\partial \boldsymbol{\lambda}}\frac{\partial \boldsymbol{\lambda}}{\partial \mathbf{F}} + \frac{\partial E_0}{\partial \mathbf{F}} \tag{3.35}$$

where the first term is zero since from Eq.(1.8), the derivatives of the energy with respect to the variational parameters are zero at the optimized parameters. The second derivative is then

$$\frac{\mathrm{d}^2E_0}{\mathrm{d}\mathbf{F}\mathrm{d}\mathbf{F}} = \frac{\partial^2 E_0}{\partial \boldsymbol{\lambda}\partial \mathbf{F}}\frac{\partial \boldsymbol{\lambda}}{\partial \mathbf{F}} + \frac{\partial^2 E_0}{\partial \mathbf{F}\partial \mathbf{F}}. \tag{3.36}$$

The second derivative of the energy is consequently a sum of two terms, the first involving the response of the wave function to the perturbation $\frac{\partial \boldsymbol{\lambda}}{\partial \mathbf{F}}$, and the second term dependent on the unperturbed wave function only. To find the response of the wave function, we use linear response theory described in Section 3.5.

3.5 Linear Response Theory

The first-order response of the wave function to an external perturbing field can be found by linear response theory. For a variational wave function, we start by differentiating the variational condition Eq.(1.8) with respect to the perturbation

$$\frac{\mathrm{d}}{\mathrm{d}\mathbf{F}}\frac{\partial E_0}{\partial \boldsymbol{\lambda}} = \frac{\partial^2 E_0}{\partial \boldsymbol{\lambda}\partial \boldsymbol{\lambda}}\frac{\partial \boldsymbol{\lambda}}{\partial \mathbf{F}} + \frac{\partial^2 E_0}{\partial \mathbf{F}\partial \boldsymbol{\lambda}} = 0. \tag{3.37}$$

Rearranging yields the response equations

$$\frac{\partial^2 E_0}{\partial \boldsymbol{\lambda}\partial \boldsymbol{\lambda}}\frac{\partial \boldsymbol{\lambda}}{\partial \mathbf{F}} = -\frac{\partial^2 E_0}{\partial \mathbf{F}\partial \boldsymbol{\lambda}}, \tag{3.38}$$

or more compactly

$$\mathbf{G}\boldsymbol{\lambda}^{\mathrm{F}} = -\mathbf{X}^{\mathrm{F}}. \tag{3.39}$$

To find the response $\boldsymbol{\lambda}^{\mathrm{F}}$ it is thus necessary to calculate the electronic Hessian $\mathbf{G}$ and the differentiated gradient $\mathbf{X}^{\mathrm{F}}$. At first sight, it might be tempting to rewrite the response equations in the form $\boldsymbol{\lambda}^{\mathrm{F}} = -\mathbf{G}^{-1}\mathbf{X}^{\mathrm{F}}$ to solve the equations. The inversion of the electronic Hessian is however a time consuming task and becomes impossible when the number of variational parameters becomes large. Therefore, the response equations are solved iteratively using the conjugate-gradient method avoiding the inversion of the large Hessian matrix.

Magnetic perturbations that give rise to imaginary singlet perturbations to the wave function (magnetizabilities, shielding constants, spin–rotation constants and rotational g-tensors) require only the knowledge of the imaginary part $\mathbf{G}^{\mathrm{i}}$ of the electronic Hessian in Eq.(3.39)—that is,

$$\left\{\mathbf{G}^{\mathrm{i}}\right\}_{ia,jb} = \frac{\partial^2 E}{\partial\lambda^{\mathrm{i}}_{ia}\lambda^{\mathrm{i}}_{jb}}, \tag{3.40}$$

where "i" denotes that the variational parameter $\lambda^{\mathrm{i}}_{ia}$ is imaginary and the subscripts denote that the variational parameter mix the occupied orbital ϕ_i with the unoccupied orbital ϕ_a. In DFT, when the exchange–correlation potential is multiplicative, the imaginary part of the electronic Hessian has a simple diagonal form and can be constructed from the orbital energies [50, 66].

$$\left\{\mathbf{G}^{\mathrm{DFT,i}}\right\}_{ia,jb} = (\epsilon_a - \epsilon_i)\,\delta_{ia,jb} \tag{3.41}$$

The solution of the response equations Eq.(3.39) is in this case simple and require only one iteration. The situation for real perturbations, arising for example from electric fields and also for the real triplet perturbations of spin–spin coupling constants, is more complicated since the real part of the Hessian is not diagonal.

In addition, for the real perturbations, the evaluation of the electronic Hessian requires the knowledge of the derivative of the exchange–correlation potential. For this reason, the calculation of spin–spin coupling constants using OEP or DCP methods is much more complicated than for the imaginary perturbations. Indeed, only imaginary second-order properties have been calculated with such potentials since here, only the undifferentiated exchange–correlation potential is needed (although polarizabilities have been calculated using finite difference methods [67, 68]). The development of analytical differentiated OEP potentials should be possible, and it will be interesting to see their application to indirect spin–spin coupling constants and electric properties in the future.

3.6 Perturbation Theory

Expressions for the energy derivatives may also be found by perturbation theory. For a set of exact states $\psi_n = |n\rangle$ (for which Eq.(1.1) holds) with energies E_n the expressions for the derivatives of the ground state energies are

$$\frac{\mathrm{d}E}{\mathrm{d}\mathbf{F}} = \langle 0 \left| \frac{\mathrm{d}H}{\mathrm{d}\mathbf{F}} \right| 0 \rangle \tag{3.42}$$

$$\frac{\mathrm{d}^2E}{\mathrm{d}\mathbf{F}^2} = \langle 0 \left| \frac{\mathrm{d}^2H}{\mathrm{d}\mathbf{F}^2} \right| 0 \rangle - 2\sum_{n\neq 0} \frac{\langle 0 \left| \frac{\mathrm{d}H}{\mathrm{d}\mathbf{F}} \right| n\rangle \langle n \left| \left(\frac{\mathrm{d}H}{\mathrm{d}\mathbf{F}}\right)^{\mathrm{T}} \right| 0\rangle}{E_n - E_0} \tag{3.43}$$

where 0 denotes the ground state and the sum is over all excited states of appropriate symmetry. In Eq.(3.43), the first term on the right is known as the diamagnetic contribution and the second term as the paramagnetic contribution. The different properties are found by inserting the appropriate derivatives of the Hamiltonian operator, Eq.(3.11). The derivatives are

$$\frac{\mathrm{d}H}{\mathrm{d}\mathbf{B}} = \mathbf{h}^{\mathrm{orb}} + \mathbf{h}^{\mathrm{spn}} = \frac{1}{2}\mathbf{L}_{\mathrm{O}} + \sum_i \mathbf{m}_i \tag{3.44}$$

$$\frac{\mathrm{d}H}{\mathrm{d}\mathbf{J}} = \mathbf{h}^{\mathrm{rot}} = -\mathbf{I}_{\mathrm{n}}^{-1} \cdot \mathbf{L}_{\mathrm{CM}} \tag{3.45}$$

$$\frac{\mathrm{d}H}{\mathrm{d}\mathbf{M}_K} = \mathbf{h}_K^{\mathrm{pso}} + \mathbf{h}_K^{\mathrm{sd}} + \mathbf{h}_K^{\mathrm{fc}} = \alpha^2 \sum_i \frac{\mathbf{l}_{iK}}{r_{iK}^3} - \alpha^2 \sum_i \mathbf{m}_i \frac{r_{iK}^2\mathbf{I}_3 - 3\mathbf{r}_{iK}\mathbf{r}_{iK}^{\mathrm{T}}}{r_{iK}^5} + \frac{8\pi\alpha^2}{3}\sum_i \mathbf{m}_i \delta\left(\mathbf{r}_{iK}\right) \tag{3.46}$$

$$\frac{\mathrm{d}^2H}{\mathrm{d}\mathbf{B}\mathrm{d}\mathbf{B}} = \mathbf{h}^{\mathrm{dma}} + \mathbf{h}^{\mathrm{nma}} = \frac{1}{4}\left(\sum_i r_{i\mathrm{O}}^2\mathbf{I}_3 - \mathbf{r}_{i\mathrm{O}}\mathbf{r}_{i\mathrm{O}}^{\mathrm{T}}\right) + \frac{1}{4}\sum_K \frac{Z_K^2}{M_K}\left(r_{K,\mathrm{CM}}^2\mathbf{I}_3 - \mathbf{r}_{K,\mathrm{CM}}\mathbf{r}_{K,\mathrm{CM}}^{\mathrm{T}}\right) \tag{3.47}$$

$$\frac{\mathrm{d}^2H}{\mathrm{d}\mathbf{B}\mathrm{d}\mathbf{J}} = \mathbf{h}^{\mathrm{nrot}} = -\frac{1}{2}\sum_K \left(Z_K r_{K,\mathrm{CM}}^2\mathbf{I}_3 - \mathbf{r}_{K,\mathrm{CM}}\mathbf{r}_{K,\mathrm{CM}}^{\mathrm{T}}\right)\mathbf{I}_{\mathrm{n}}^{-1} \tag{3.48}$$

$$\frac{\mathrm{d}^2H}{\mathrm{d}\mathbf{B}\mathrm{d}\mathbf{M}_K} = \mathbf{h}_K^{\mathrm{dsh}} - \mathbf{1} = \frac{\alpha^2}{2}\sum_i \left(\frac{\mathbf{r}_{i\mathrm{O}}\cdot\mathbf{r}_{iK}\mathbf{I}_3 - \mathbf{r}_{iK}\mathbf{r}_{i\mathrm{O}}^{\mathrm{T}}}{r_{iK}^3}\right) - \mathbf{1} \tag{3.49}$$

$$\frac{\mathrm{d}^2H}{\mathrm{d}\mathbf{J}\mathrm{d}\mathbf{J}} = \mathbf{h}^{\mathrm{ine}} = \mathbf{I}_{\mathrm{n}}^{-1} \tag{3.50}$$

$$\frac{\mathrm{d}^2H}{\mathrm{d}\mathbf{J}\mathrm{d}\mathbf{M}_K} = \mathbf{h}_K^{\mathrm{nsr}} = -\frac{\alpha^2}{2}\sum_{L\neq K}\frac{Z_L}{r_{KL}^3}\left(r_{KL}^2\mathbf{I}_3 - \mathbf{r}_{KL}\mathbf{r}_{KL}^{\mathrm{T}}\right)\mathbf{I}_{\mathrm{n}}^{-1} \tag{3.51}$$

$$\frac{\mathrm{d}^2H}{\mathrm{d}\mathbf{M}_K\mathrm{d}\mathbf{M}_L} = \mathbf{D}_{\mathbf{KL}} + \mathbf{h}_{KL}^{\mathrm{dso}} = \frac{1}{2}\sum_K\sum_{L\neq K}\frac{r_{KL}^2\mathbf{I}_3 - 3\mathbf{r}_{KL}\mathbf{r}_{KL}^{\mathrm{T}}}{r_{KL}^5} + \frac{\alpha^4}{2}\sum_i \frac{\left(\mathbf{r}_{iK}\cdot\mathbf{r}_{iL}\right)\mathbf{I}_3 - \mathbf{r}_{iK}\mathbf{r}_{iL}^{\mathrm{T}}}{r_{iK}^3 r_{iL}^3}. \tag{3.52}$$

The perturbation-theory expressions Eqs.(3.42) and (3.43) illustrate better than do the expressions of Section 3.4 the mechanisms responsible for the energy derivatives and properties in terms of the ground state, the excited states and operators. They are, however, not useful for practical calculations since explicit expressions for all the excited states are needed. In the next sections, the explicit perturbation expressions will be given for each property to illustrate which mechanisms are responsible for the different properties.

3.7 Qualitative Description of Magnetic Properties

In this Section, a qualitative description of the molecular properties defined in Section 3.1 is presented. First, the rotational g-tensor is considered in Section 3.7.1 followed by the magnetizability in Section 3.7.2. Then, the close relation between the rotational g-tensor and the magnetizability is shown in Section 3.7.3. The NMR shielding constant, the spin-rotation constant and their relation are presented in Sections 3.7.4, 3.7.5 and 3.7.6, respectively. The indirect NMR spin–spin coupling constant is finally treated in Section 3.7.7.

3.7.1 The Rotational g-tensor

The rotational g-tensor term in Eq.(3.4) describes the interaction energy between the magnetic moment set up by a rotating molecule

$$\boldsymbol{\mu}_{\mathrm{rot}} = \mu_{\mathrm{n}} \mathbf{J}^{\mathrm{T}} \mathbf{g} \tag{3.53}$$

and an external magnetic field $\mathbf{B}$ [56, 69]. The rotational g-tensor may be split into two terms, a positive contribution arising from the rotation of the nuclei $\mathbf{g}^{\mathrm{n}}$ and a negative contribution from the rotation of the electrons $\mathbf{g}^{\mathrm{e}}$

$$\mathbf{g} = \mathbf{g}^{\mathrm{e}} + \mathbf{g}^{\mathrm{n}}. \tag{3.54}$$

Inserting the operators of Eqs.(3.44), (3.45) and (3.48) into the second-order perturbation expression of Eq.(3.43), the g-tensor can be evaluated as

$$\mathbf{g} = -\frac{1}{\mu_{\mathrm{n}}} \langle 0 \left| \mathbf{h}^{\mathrm{nrot}} \right| 0 \rangle + \frac{2}{\mu_{\mathrm{n}}} \sum_{n_{\mathrm{S}} \neq 0} \frac{\langle 0 \left| \mathbf{h}^{\mathrm{orb}} \right| n_{\mathrm{S}} \rangle \langle n_{\mathrm{S}} \left| \left(\mathbf{h}^{\mathrm{rot}} \right)^{\mathrm{T}} \right| 0 \rangle}{E_{n_{\mathrm{S}}} - E_0}. \tag{3.55}$$

Since in the diamagnetic term, $\mathbf{h}^{\mathrm{nrot}}$ is only dependent on the nuclear coordinates, the operator may be taken outside the integral yielding the nuclear contribution to

the g-tensor $\mathbf{g}^{\mathrm{n}} = -\frac{1}{\mu_{\mathrm{n}}}\mathbf{h}^{\mathrm{nrot}}$. In the paramagnetic contribution, which is equal to the electronic contribution $\mathbf{g}^{\mathrm{e}}$, there is no contribution from total electron spin operator $\mathbf{h}^{\mathrm{spn}}$ from Eq.(3.44) since this operator, when working on the closed shell ground state gives zero. The operators $\mathbf{h}^{\mathrm{orb}}$ and $\mathbf{h}^{\mathrm{rot}}$ give singlet states when they operate on the closed shell ground state. It is therefore only necessary to consider singlet excited states n_{S} in the summation of Eq.(3.55).

In experiment, the interaction between the rotational magnetic moment and an external magnetic field can be observed as a Zeeman splitting of the rotational spectrum in molecular beam and microwave spectroscopy, that is, it appears as a shift in the rotational spectrum when a magnetic field is present. From these measurements, it is possible to determine all the diagonal elements of the rotational g-tensor.

The accuracy of measurements in microwave spectroscopy is impressive, up to 10 significant digits can nowadays be recorded in the resonance frequencies. This accuracy is also reflected in the accuracy of measured rotational g-tensors. For diamagnetic molecules, experimental error bars are very small, usually below 0.1% of the total g-tensor element. Thus, the rotational g-tensor is particularly attractive for testing theoretical models against experiment. In addition to providing accurate measurements, the experiments are done in the gas phase. This means that it is not necessary to consider solvation effects in the quantum chemical calculations. Rotational effects are also small as the measured g-tensor is obtained from transitions between known rotational states of low angular momentum, in many cases from the $J = 0 \rightarrow 1$ transition. To compare calculations to experiment, it is therefore not necessary to consider ensembles of rotational states at a given temperature. So, provided that the effects of zero point vibrations on the g-tensor elements are small, the bare experimentally measured g-tensors provide an accurate benchmark data set to assess the performance of different quantum chemistry models.

3.7.2 The Magnetizability

The magnetizability describes the second-order response of the molecule to an external magnetic field. Inserting Eqs.(3.44) and (3.47) into Eq.(3.43), we obtain for the magnetizability tensor

$$\boldsymbol{\xi} = -\langle 0 \left| \mathbf{h}^{\mathrm{dma}} \right| 0 \rangle + 2 \sum_{n_{\mathrm{S}} \neq 0} \frac{\langle 0 \left| \mathbf{h}^{\mathrm{orb}} \right| n_{\mathrm{S}} \rangle \langle n_{\mathrm{S}} \left| \left(\mathbf{h}^{\mathrm{orb}} \right)^{\mathrm{T}} \right| 0 \rangle}{E_{n_{\mathrm{S}}} - E_0}. \tag{3.56}$$

The nuclear contribution $\mathbf{h}^{\mathrm{nma}}$ in Eq.(3.47) is neglected as it is small [56] and also does not contribute to the magnetizability for a non-rotating molecule within the Born–Oppenheimer approximation. In the paramagnetic term, $\mathbf{h}^{\mathrm{spn}}$ from Eq.(3.44) vanishes when working on the ground-state closed-shell wave function.

The isotropic magnetizability is the average of the diagonal magnetizability tensor elements

$$\xi^{\mathrm{iso}} = \frac{1}{3}\mathrm{Tr}\boldsymbol{\xi} \tag{3.57}$$

The direct measurement of the magnetizability is made difficult for several reasons. In gas phase, a very low oxygen contamination of the sample may influence the measurement significantly. In addition, there are difficulties related to the calibration standards used in the experiments. Together these effects lead to large experimental error bars for the isotropic magnetizability [70]. In addition to experimental difficulties, measurements are often done in the liquid phase which are not directly comparable to calculated magnetizabilities of single molecules. Solvation effects must therefore be taken into account for the comparison between experiment and theory. In summary, experimental magnetizabilities do not provide good data for benchmarking purposes.

More accurate measurements of the magnetizability may be obtained from microwave spectroscopy, however, only two independent magnetizability tensor components, that is the magnetizability anisotropies, may be observed directly by experiment [71]. If the moment of inertia is known for the molecule, then the paramagnetic contribution to the individual diagonal tensor elements may be derived. The independent diagonal elements of the total magnetizability can then be obtained in a semi-experimental manner by adding a theoretically derived diamagnetic contribution to the magnetizability tensor.

3.7.3 Relation Between the g-tensor and the Magnetizability

The g-tensor and the magnetizability are closely related properties. In fact, the electronic contribution to the g-tensor can be derived from the paramagnetic magnetizability and vice versa since the effect of a magnetic field on a system of electrons is proportional to the effect of a molecular rotation [69]. This similarity is also reflected in the operators $\mathbf{h}^{\mathrm{orb}}$ and $\mathbf{h}^{\mathrm{rot}}$ when the gauge origin of $\mathbf{h}^{\mathrm{orb}}$ is placed at the center of mass

$$\mathbf{h}^{\mathrm{rot}} = -2\mathbf{I}_{\mathrm{n}}^{-1}\mathbf{h}_{\mathrm{CM}}^{\mathrm{orb}} \tag{3.58}$$

The relation between the electronic part of the rotational g-tensor and the magnetizability is [56]

$$g^{\mathrm{e}}_{xx} = -\frac{4M_{\mathrm{p}}}{I_{xx}}\xi^{\mathrm{p}}_{xx} \tag{3.59}$$

where ξ^{p} is the paramagnetic magnetizability and the proton mass is M_{p}.

The relation Eq.(3.59) takes the following form when using rotational London atomic orbitals [62]

$$\mathbf{g} = -4M_{\mathrm{p}}\left(\boldsymbol{\xi}^{\mathrm{LAO}} - \boldsymbol{\xi}^{\mathrm{d}}\left(\mathrm{CM}\right)\right)\mathbf{I}_{\mathrm{n}}^{-1} + \mathbf{g}^{\mathrm{n}}. \tag{3.60}$$

The LAO denotes that the total magnetizability $\boldsymbol{\xi}^{\mathrm{LAO}}$ has been calculated using London atomic orbitals, whereas $\boldsymbol{\xi}^{\mathrm{d}}\left(\mathrm{CM}\right)$ is the diamagnetic contribution to the magnetizability calculated without London atomic orbitals and with the gauge origin at the center of mass.

3.7.4 The Shielding Constant

The nuclear shielding constant is of great importance in chemistry, used in molecular structure determination in nuclear magnetic resonance (NMR) spectroscopy. The shielding constant is a result of the interaction between an external magnetic field and the magnetic moment of the nucleus. This interaction is determined by the strength of the magnetic field at the nucleus which consists of the external magnetic field modified by the magnetic field set up by the electrons. The shielding constant describes the modification of the magnetic field at the nucleus due to the electronic motions.

Using Eqs.(3.8), (3.44), (3.46), (3.49) and (3.43), the perturbation expression for the shielding constant is

$$\boldsymbol{\sigma}_K = \langle 0 \left| \mathbf{h}^{\mathrm{dsh}}_K \right| 0 \rangle - 2\sum_{n_{\mathrm{S}}\neq 0} \frac{\langle 0 \left| \mathbf{h}^{\mathrm{orb}} \right| n_{\mathrm{S}} \rangle \langle n_{\mathrm{S}} \left| \left(\mathbf{h}^{\mathrm{pso}}_K\right)^{\mathrm{T}} \right| 0 \rangle}{E_{n_{\mathrm{S}}} - E_0}. \tag{3.61}$$

In the paramagnetic contribution, the $\mathbf{h}^{\mathrm{orb}}$ is the only surviving part of Eq.(3.44) since $\mathbf{h}^{\mathrm{spn}}|0>=0$. The $\mathbf{h}^{\mathrm{orb}}$ operator generates singlet imaginary states and couples only to the singlet imaginary generating $\mathbf{h}^{\mathrm{pso}}_K$ operator of Eq.(3.46). The $\mathbf{h}^{\mathrm{sd}}_K$ and $\mathbf{h}^{\mathrm{fc}}_K$ operators give real triplet states when acting on the ground state and do not couple with $\mathbf{h}^{\mathrm{orb}}$.

The isotropic shielding constant is

$$\sigma_K = \frac{1}{3}\mathrm{Tr}\boldsymbol{\sigma}_K \tag{3.62}$$

In the NMR experiment, the chemical shift δ_K relative to a reference nucleus is observed

$$\delta_K = \sigma_K - \sigma_{\mathrm{ref}}. \tag{3.63}$$

The chemical shifts can be determined to good accuracy in experiment with uncertainties of around 0.01 ppm. The accuracy of the measured isotropic shielding constant on an absolute scale is lower—the accuracy is restricted by the accuracy of the reference σ_{ref}, relative to the bare nucleus in question. The accuracy to which σ_{ref} is known varies among nucleus types, usually the accuracy is lower for heavier nuclei. Wave function methods can be used to obtain σ_{ref}, however, to be useful in experimental measurements, the calculated σ_{ref} must account for solvation and ro-vibrational effects valid for the particular experimental setup, and also relativistic effects for heavy nuclei. The calculation of σ_{ref} is therefore a challenging task.

The paramagnetic contribution to the absolute shielding of Eq.(3.62) can be determined accurately in experiment from measurements on the spin–rotation constant, see Section 3.7.6. An alternative for obtaining the total absolute shielding of a nucleus is then to calculate the diamagnetic contribution from theory and add the experimental paramagnetic contribution.

Although there are some NMR experiments that have been performed in the gas phase, most measurements are done in liquid and solid state. The limited amount of gas phase data makes it necessary to consider liquid phase experiments when comparing to calculated numbers. For a critical comparison with experiment therefore, both solvation and ro-vibrational effects should be accounted for in the calculations.

3.7.5 The Spin-Rotation Constant

The spin-rotation constant describes the interaction between the magnetic moment of the nucleus and the magnetic field arising from the rotational motion of the molecule. As for the g-tensor, the spin-rotation constant may be separated into nuclear and electronic contributions

$$\mathbf{C}_K = \mathbf{C}_K^{\text{e}} + \mathbf{C}_K^{\text{n}}. \tag{3.64}$$

Inserting the perturbation expression Eq.(3.43) with the operators Eqs.(3.51), (3.45), (3.46) in the spin–rotation constant expression Eq.(3.7), we obtain

$$\mathbf{C}_K = -\langle 0 \left| \mathbf{h}_K^{\text{nsr}} \right| 0 \rangle + 2 \sum_{n_{\text{S}} \neq 0} \frac{\langle 0 \left| \mathbf{h}^{\text{rot}} \right| n_{\text{S}} \rangle \langle n_{\text{S}} \left| \left(\mathbf{h}_K^{\text{pso}} \right)^{\text{T}} \right| 0 \rangle}{E_{n_{\text{S}}} - E_0}. \tag{3.65}$$

and the diamagnetic contribution reduces to the nuclear contribution $\mathbf{C}_K^{\text{n}} = -\mathbf{h}_K^{\text{nsr}}$ as the $\mathbf{h}_K^{\text{nsr}}$ operator is only dependent on the nuclear coordinates. In the paramagnetic contribution, as for the shielding constant, only $\mathbf{h}_K^{\text{pso}}$ in Eq.(3.46) has the correct symmetry for coupling to $\mathbf{h}^{\text{rot}}$, therefore $\mathbf{h}_K^{\text{fc}}$ and $\mathbf{h}_K^{\text{sd}}$ do not appear in Eq.(3.65). The

experimental measurement of spin–rotation constants can be performed with good accuracy in microwave spectroscopy.

3.7.6 Relation Between the Spin-Rotation Tensor and the Shielding Tensor

A similar relation is found between the spin-rotation constant and the shielding tensor as with the rotational g-tensor and the magnetizability Eq.(3.59). The electronic part of the spin-rotation tensor is related to the paramagnetic contribution to the shielding constant

$$C^{\mathrm{e}}_{K,xx} = 2\gamma_K \sigma^{\mathrm{p}}_{K,xx} I^{-1}_{xx} \tag{3.66}$$

where γ_K is the gyromagnetic ratio of the Kth nucleus. When using rotational London atomic orbitals, the relation between the spin–rotation constant and the shielding constants is [62]

$$\mathbf{C}_K = 2\gamma_K(\boldsymbol{\sigma}^{\mathrm{LAO}}_K - \boldsymbol{\sigma}^{\mathrm{d}}_K(\mathbf{r}_K))\mathbf{I}^{-1}_{\mathrm{n}} + \mathbf{C}^{\mathrm{n}}_K \tag{3.67}$$

where $\boldsymbol{\sigma}^{\mathrm{d}}_K(\mathbf{r}_K)$ is the diamagnetic contribution to the shielding tensor calculated using conventional basis functions with the gauge origin at the nucleus K and $\boldsymbol{\sigma}^{\mathrm{LAO}}_K$ is the total shielding constant calculated using London atomic orbitals.

3.7.7 The Indirect Nuclear Spin–Spin Coupling Constant

The NMR spin–spin coupling constant is the second parameter, in addition to the shielding constant, that is responsible for the resonance pattern in NMR spectroscopy. It describes the interaction of the magnetic moments of the nuclei. This interaction can be of a direct nature—that is, a magnetic dipole–dipole interaction between the two magnetic moments of the nuclei, or of an indirect nature mediated by the magnetic moments of the electrons due to their spin. The much larger direct dipole–dipole interaction cancels out in a gas or liquid phase NMR experiments as a result of the rotational movement of the molecules. Therefore, the spin–spin coupling constant observed in gas and liquid phase experiment is the indirect nuclear spin–spin coupling constant.

Using the definition of the reduced indirect nuclear spin–spin coupling constant Eq.(3.9), and inserting Eqs.(3.46) and (3.52) into the second-order perturbation expression Eq.(3.43), the reduced indirect nuclear spin–spin coupling constant is found

to be

$$\begin{aligned}\mathbf{K}_{KL} &= -\langle 0 \left|\mathbf{h}_{KL}^{\mathrm{dso}}\right| 0\rangle + 2\sum_{n_{\mathrm{S}}\neq 0} \frac{\langle 0 \left|\mathbf{h}_{K}^{\mathrm{pso}}\right| n_{\mathrm{S}}\rangle\langle n_{\mathrm{S}} \left|\left(\mathbf{h}_{L}^{\mathrm{pso}}\right)^{\mathrm{T}}\right| 0\rangle}{E_{n_{\mathrm{S}}} - E_0} \\ &\quad +2\sum_{n_{\mathrm{T}}\neq 0} \frac{\langle 0 \left|\mathbf{h}_{K}^{\mathrm{sd}} + \mathbf{h}_{K}^{\mathrm{fc}}\right| n_{\mathrm{T}}\rangle\langle n_{\mathrm{T}} \left|\left(\mathbf{h}_{L}^{\mathrm{sd}}\right)^{\mathrm{T}} + \left(\mathbf{h}_{L}^{\mathrm{fc}}\right)^{\mathrm{T}}\right| 0\rangle}{E_{n_{\mathrm{T}}} - E_0}. \end{aligned} \tag{3.68}$$

The sum over states terms are separated into sums over singlet states n_{S} and triplet states n_{T} reflecting the singlet symmetry of the states that result when the $\mathbf{h}_K^{\mathrm{pso}}$ operator act on the closed shell ground state and the triplet symmetry of the states that result from $\mathbf{h}_K^{\mathrm{sd}}$ and $\mathbf{h}_K^{\mathrm{fc}}$. The diamagnetic part of Eq.(3.68) is the diamagnetic spin-orbit (DSO) contribution, the sum over singlet states is the paramagnetic spin-orbit (PSO) contribution and the sum over triplet states constitutes the spin-dipolar (SD) and Fermi-contact (FC) contributions to the spin–spin coupling constant.

The indirect nuclear spin–spin coupling tensor $\mathbf{J}_{KL}$ that is usually reported in the literature is related to the reduced tensor $\mathbf{K}_{KL}$ by

$$\mathbf{J}_{KL} = h\frac{\gamma_K}{2\pi}\frac{\gamma_L}{2\pi}\mathbf{K}_{KL}. \tag{3.69}$$

where γ_K is the gyromagnetic ratio of nucleus K and h is the Planck constant. The isotropic spin–spin coupling constant is

$$J_{KL} = \frac{1}{3}\mathbf{Tr}\mathbf{J}_{KL} \tag{3.70}$$

Due to the presence of the triplet operators $\mathbf{h}_K^{\mathrm{sd}}$ and $\mathbf{h}_K^{\mathrm{fc}}$, the spin–spin coupling constant stand out as different to the other properties studied in this thesis. For a good description of the spin–spin coupling constant, also the triplet states must be well described by the theoretical model. Triplet states at the Hartree–Fock level of theory are poorly described due to triplet instabilities—the model predicts erroneously low energy triplet states or even negative triplet excitation energies. The result is that predictions of spin–spin coupling constants using Hartree–Fock theory are meaningless. Since DFT show triplet instabilities to a much smaller extent, DFT is the only successful low cost alternative for calculations of indirect spin–spin coupling constants.

The experimental accuracy of spin–spin coupling constants varies a lot with the nucleus types that are coupled. Nuclei having a spin $\mathbf{I}_K$ larger than $\frac{1}{2}$, give broad resonance peaks in the NMR spectra, and the spin–spin coupling becomes hard to measure accurately. As for the NMR shielding constants, measurements are usually done in liquid phase and solvation effects together with ro-vibrational effects must be accounted for when comparing the results to calculated spin–spin coupling constants.

Chapter 4

Ro-vibrational Effects

Property calculations that are performed within the Born–Oppenheimer approximation are valid for non-vibrating, non-rotating molecules. However, even at a temperature of 0 K, molecules will exhibit zero-point vibrations (ZPV). Depending on the type of property and the molecule, the rotational and vibrational motion will affect the value of the property to different degrees. In some cases, the ro-vibrational effects are highly significant. Therefore, for a critical comparison with experiment, it is important to consider the ro-vibrational effects.

In this Chapter, we will outline the theory for calculation of vibrational corrections used in this thesis. Some general considerations are given in Section 4.1, then the approaches used in this work are described in Section 4.2.

4.1 General Considerations

In the Born–Oppenheimer approximation, the nuclear positions are treated as parameters, and all properties P, including the energy, are functions of the nuclear geometry

$$P = P(\mathbf{R}), \tag{4.1}$$

where $\mathbf{R}$ represents a nuclear geometry. If the property in question is the energy, $P(\mathbf{R})$ becomes the potential energy surface. To account for the effect of nuclear motion on the properties, it is necessary to average $P(\mathbf{R})$ over the nuclear wave function $\Psi_{\mathrm{n},i}(\mathbf{R})$ (defined later). At a temperature of 0K the averaging can be performed over the ground-state nuclear wave function $\Psi_{\mathrm{n},0}(\mathbf{R})$

$$P_{\mathrm{ave},0} = \langle \Psi_{\mathrm{n},0}(\mathbf{R}) | P(\mathbf{R}) | \Psi_{\mathrm{n},0}(\mathbf{R}) \rangle, \tag{4.2}$$

where the integration is over the nuclear coordinates. The ground-state nuclear wave function describes the zero point vibrations of the molecule. The zero-point vibrational contribution (ZPVC) to the property, P_{ZPVC}, is

$$P_{\mathrm{ZPVC}} = P_{\mathrm{ave},0} - P_{\mathrm{eq}} \tag{4.3}$$

where the property calculated at the equilibrium geometry within the Born–Oppenheimer approximation, P_{eq}, has been subtracted from the vibrationally averaged property $P_{\mathrm{ave},0}$. For temperatures above 0K, the vibrational averaging must include excited states of the nuclear wave function through a Boltzmann averaging.

The nuclear wave functions are the solutions to the nuclear Schrödinger equation

$$\left[-\sum_K \frac{\nabla_K^2}{2M_K} + V_{\mathrm{PES}}(\mathbf{R}) \right] \Psi_{\mathrm{n},i}(\mathbf{R}) = E_{\mathrm{n},i} \Psi_{\mathrm{n},i}(\mathbf{R}) \tag{4.4}$$

where $V_{\mathrm{PES}}(\mathbf{R})$ is the potential energy surface and i is a label to distinguish the nuclear wave function states and the corresponding energies $E_{\mathrm{n},i}$. The first term in the square brackets, the kinetic energy operator, takes different forms depending on which coordinate system is used to describe the nuclear motion, see for example Ref. [72]. Having found a representation of the kinetic energy operator and the potential energy surface, the nuclear vibrational wave function may be obtained in different ways for example using a variational self consistent field wave function [73] or other variational methods [72].

A different approach than the variational method is to find the vibrational wave function from perturbation theory, as used in this thesis [74, 75, 76, 77, 78]. The applicability of this approach is more limited compared to the variational treatment — the vibrations must not have so large amplitudes that the perturbation theory breaks down. The perturbation treatment is however still useful for the calculation of ZPVC to molecular properties provided that the vibrations do not cause very large nuclear displacements. In Section 4.2, two approaches based on the perturbation treatment that have been employed in this work will be described.

Another alternative is to treat the vibrational effects directly using the full non-Born–Oppenheimer Schrödinger equation Eq.(1.1) with the Hamiltonian Eq.(1.2) treating the nuclei and electrons on an equal footing. The ro-vibrational motion of the nuclei is then an integral part of the wave function, and the vibrational contribution can not be considered separate from the electronic contribution. These calculations are however very expensive and only applied to very small molecules like H_2 and LiH [79, 80].

4.2 Perturbation Expansion Treatment

The vibrational wave function and the ZPVC to properties can be obtained using perturbation theory. Here, we express the nuclear motions in normal coordinates Q_k at the molecular equilibrium geometry. In normal coordinates, the harmonic oscillator Hamiltonian can be separated into a sum of Hamiltonians, one for each coordinate [81]

$$H^{\text{harmonic}} = \frac{1}{2}\sum_k \left(-\frac{\partial^2}{\partial Q_k^2} + \kappa_k Q_k^2\right) \tag{4.5}$$

where κ_k are the force constants and the sum runs over the $3K$ normal coordinates, K being the number of nuclei. Six (five for linear molecules) of the normal coordinates correspond to translation and rotation of the molecule and there are consequently $3K-6(5)$ vibrational normal coordinates in the harmonic approximation. The eigenvalues $E_{\mathbf{k}}$ of the Hamiltonian Eq.(4.5) are sums of harmonic oscillator eigenvalues E_k

$$E_{\mathbf{k}} = \sum_k E_k = \sum_k \left(n_k + \frac{1}{2}\right)\omega_k \tag{4.6}$$

where the vibrational frequencies $\omega_k = \sqrt{\kappa_k}$ and $n_k = 0, 1, 2, \ldots$ are quantum numbers specifying the vibrational state of the k'th normal mode. The eigenfunctions, $\Psi^{\text{harmonic}}_{\text{n},\mathbf{k}}$ of Eq.(4.5) are products of harmonic oscillator wave functions written in terms of Hermite polynomials $H_{n_k}(Q_k)$

$$\Psi^{\text{harmonic}}_{\text{n},\mathbf{k}} = \prod_k \psi_{\text{n},k} = \prod_k N_k H_{n_k}(Q_k)\mathrm{e}^{-\frac{1}{2}Q_k^2} \tag{4.7}$$

where N_k are normalization constants. Part of the ZPVC can in fact be calculated by inputing the harmonic oscillator wavefunction Eq.(4.7) into Eq.(4.2), however, also anharmonic vibrations are important. The anharmonic contributions can be obtained from perturbation theory.

Having decided on the coordinate system in terms of normal coordinates, we continue by expanding the potential energy surface as a Taylor series around some arbitrary expansion point $\mathbf{Q}_{\text{ref}}$

$$\begin{aligned} V(\mathbf{Q}) = E(\mathbf{Q}_{\text{ref}}) &+ \sum_k \frac{\mathrm{d}E}{\mathrm{d}Q_k}\Delta Q_k + \frac{1}{2}\sum_{kl}\frac{\mathrm{d}^2E}{\mathrm{d}Q_k\mathrm{d}Q_l}\Delta Q_k\Delta Q_l \\ &+ \frac{1}{6}\sum_{klm}\frac{\mathrm{d}^3E}{\mathrm{d}Q_k\mathrm{d}Q_l\mathrm{d}Q_m}\Delta Q_k\Delta Q_l\Delta Q_m \\ &+ \frac{1}{24}\sum_{klmn}\frac{\mathrm{d}^4E}{\mathrm{d}Q_k\mathrm{d}Q_l\mathrm{d}Q_m\mathrm{d}Q_n}\Delta Q_k\Delta Q_l\Delta Q_m\Delta Q_n + \ldots \end{aligned} \tag{4.8}$$

where the electronic energy E and its derivatives are evaluated at $\mathbf{Q}_{\text{ref}}$ and $\Delta Q_k = Q_k - Q_{k,\text{ref}}$.

Using standard time-independent perturbation theory, we split the perturbed Hamiltonian, wave function and energy into orders in the perturbation

$$H = H^{(0)} + H^{(1)} + H^{(2)} + \dots \tag{4.9}$$

$$\Psi_{\text{n}} = \Psi_{\text{n}}^{(0)} + \Psi_{\text{n}}^{(1)} + \Psi_{\text{n}}^{(2)} + \dots \tag{4.10}$$

$$E = E^{(0)} + E^{(1)} + E^{(2)} + \dots \tag{4.11}$$

which, when inserted into the Schrödinger equation, results in a set of equations, one for each order

$$H^{(0)}\Psi_{\text{n}}^{(0)} = E^{(0)}\Psi_{\text{n}}^{(0)} \tag{4.12}$$

$$\left(H^{(1)} - E^{(1)}\right)\Psi_{\text{n}}^{(0)} = \left(E^{(0)} - H^{(0)}\right)\Psi_{\text{n}}^{(1)} \tag{4.13}$$

$$\left(H^{(2)} - E^{(2)}\right)\Psi_{\text{n}}^{(0)} + \left(H^{(1)} - E^{(1)}\right)\Psi_{\text{n}}^{(1)} = \left(E^{(0)} - H^{(0)}\right)\Psi_{\text{n}}^{(2)} \tag{4.14}$$

These equations may be solved to yield the perturbed energies and wave functions. The next sections describe the solution to these equations based on two different choices of the expansion point $\mathbf{Q}_{\text{ref}}$.

4.2.1 Potential Expansion Around the Equilibrium Geometry

The ZPVC obtained from expansion of the potential energy surface around the equilibrium geometry has been described by Kern and Matcha [74, 75, 76]. Expanding the potential energy surface around the equilibrium geometry, $\mathbf{Q}_{\text{ref}} = \mathbf{0}$, setting $E(\mathbf{0}) = 0$, yields

$$\begin{aligned} V(\mathbf{Q}) = {} & \frac{1}{2}\sum_k \frac{\mathrm{d}^2 E}{\mathrm{d}^2 Q_k} Q_k^2 + \frac{1}{6}\sum_{klm} \frac{\mathrm{d}^3 E}{\mathrm{d}Q_k \mathrm{d}Q_l \mathrm{d}Q_m} Q_k Q_l Q_m \\ & + \frac{1}{24}\sum_{klmn} \frac{\mathrm{d}^4 E}{\mathrm{d}Q_k \mathrm{d}Q_l \mathrm{d}Q_m \mathrm{d}Q_n} Q_k Q_l Q_m Q_n + \dots \end{aligned} \tag{4.15}$$

as the first derivative vanishes at the stationary equilibrium geometry. The second derivative of the energy is diagonal in the normal coordinates.

We can now set up the Hamiltonians

$$H^{(0)} = H^{\text{harmonic}} \tag{4.16}$$

$$H^{(1)} = \frac{1}{6}\sum_{klm} k_{klm} Q_k Q_l Q_m \tag{4.17}$$

$$H^{(2)} = \frac{1}{24}\sum_{klmn} k_{klmn} Q_k Q_l Q_m Q_n \tag{4.18}$$

where k_{klm} and k_{klmn} are the cubic and quartic force constants, respectively

$$k_{klm} = \frac{\mathrm{d}^3 E}{\mathrm{d}Q_k \mathrm{d}Q_l \mathrm{d}Q_m} \tag{4.19}$$

$$k_{klmn} = \frac{\mathrm{d}^4 E}{\mathrm{d}Q_k \mathrm{d}Q_l \mathrm{d}Q_m \mathrm{d}Q_n}. \tag{4.20}$$

The summations are over the $3N-6(5)$ vibrational normal coordinates—the rigid rotation of the nuclear framework and its coupling to the anharmonic vibrational movement is omitted from H since we are here only interested in zero point vibrations with rotational quantum number $J = 0$.

The zeroth-order ground-state wave function is, inserting Eq.(4.16) into Eq.(4.12)

$$\Psi_{\mathrm{n}}^{(0)} = \Psi_{\mathrm{n}}^{\mathrm{harmonic}}. \tag{4.21}$$

To construct the first order wave function, consider a general virtual excitation from $\Psi_{\mathrm{n}}^{\mathrm{harmonic}}$

$$\Psi_{abc\ldots}^{rst\ldots} \tag{4.22}$$

where the excitation levels of normal mode $a, b, c \ldots$ in $\Psi_{\mathrm{n}}^{\mathrm{harmonic}}$ has been replaced by the excitation levels $r, s, t, \ldots$. The first order wave function is expanded in all possible virtual excitations from $\Psi_{\mathrm{n}}^{\mathrm{harmonic}}$

$$\Psi_{\mathrm{n}}^{(1)} = \sum_a \sum_r^{\infty} \alpha_{ar}^{(1)} \Psi_a^r + \sum_{ab} \sum_{rs}^{\infty} \beta_{abrs}^{(1)} \Psi_{ab}^{rs} + \sum_{abc} \sum_{rst}^{\infty} \gamma_{abcrst}^{(1)} \Psi_{abc}^{rst} + \ldots \tag{4.23}$$

where $\alpha_{ar}^{(1)}, \beta_{abrs}^{(1)}$ and $\gamma_{abcrst}^{(1)}$ are expansion coefficients. The first order expansion coefficients are found by solving the second-order perturbation equation. The result, when truncating H at $H^{(2)}$, is that only four types of coefficients do not vanish [74]

$$\alpha_{a1}^{(1)} = -\frac{1}{4\sqrt{2}\left(\omega_a\right)^{3/2}} \sum_b \frac{k_{abb}}{\omega_b} \tag{4.24}$$

$$\alpha_{a3}^{(1)} = -\frac{\sqrt{3}}{36\left(\omega_a\right)^{5/2}} k_{aaa} \tag{4.25}$$

$$\beta_{ab21}^{(1)} = -\frac{1}{4\omega_a\sqrt{\omega_b}} \frac{k_{aab}}{2\omega_a + \omega_b} \tag{4.26}$$

$$\gamma_{abc111}^{(1)} = -\frac{\sqrt{1}}{12\sqrt{2\omega_a\omega_b\omega_c}} \frac{k_{abc}}{\omega_a + \omega_b + \omega_c} \tag{4.27}$$

The force constants in these equations may be calculated by analytical derivative techniques as in linear response theory (for harmonic frequencies), by numerical methods or a combination of both. The expressions here in normal coordinates using a Taylor

expansion of the PES look different from the expressions in Ref. [74] where the equations are expressed in *reduced* normal coordinates and a power series is used instead of a Taylor series for the PES.

Having obtained a form of the nuclear wave function, truncating Eq.(4.10) at $\Psi_{\mathrm{n}}^{(1)}$, we proceed by expressing the property as a function of the nuclear coordinates in a Taylor series in the normal coordinates

$$P = P_0 + \sum_k \alpha_k Q_k + \frac{1}{2}\sum_{kl} \beta_{kl} Q_k Q_l + \frac{1}{6}\sum_{klm} \gamma_{klm} Q_k Q_l Q_m \dots \tag{4.28}$$

where P_0 is the equilibrium geometry value for the property and α_k, β_{kl} and γ_{klm} are expansion coefficients determined as first, second and third derivatives with respect to normal mode displacements of the nuclei, respectively—for example, $\alpha_k = \frac{\mathrm{d}P}{\mathrm{d}Q_k}$.

Inserting Eqs.(4.10) and (4.28) in to Eq.(4.2), the ZPVC can be calculated as [74]

$$P_{\mathrm{ZPVC}} = \frac{1}{4}\sum_k \frac{1}{\omega_k}\frac{\mathrm{d}^2 P}{\mathrm{d}Q_k^2} - \frac{1}{4}\sum_k \frac{1}{\omega_k^2}\frac{\mathrm{d}P}{\mathrm{d}Q_k}\sum_l \frac{k_{kll}}{\omega_l}. \tag{4.29}$$

To obtain the ZPVC, it is therefore necessary to calculate the first derivative and the diagonal part of the second derivative of the property with respect to normal coordinates as well as the vibrational frequencies and the semi-diagonal part of the cubic force field.

4.2.2 Potential Expansion Around an Effective Geometry

In a different but related approach that is used to determine ZPVCs in this thesis, the property and potential surface expansions are not done around the equilibrium geometry but around a variationally determined effective geometry [77, 78]. The effective geometry is found by minimizing the function

$$\tilde{E}(\mathbf{Q}_{\mathrm{ref}}) = E_0(\mathbf{Q}_{\mathrm{ref}}) + \langle \Psi_{\mathrm{n}} \left| H^{(0)}(\mathbf{Q}_{\mathrm{ref}}) \right| \Psi_{\mathrm{n}} \rangle = E_0(\mathbf{Q}_{\mathrm{ref}}) + \frac{1}{2}\sum_k \omega_k(\mathbf{Q}_{\mathrm{ref}}) \tag{4.30}$$

with respect to the expansion point $\mathbf{Q}_{\mathrm{ref}}$. The effective geometry corresponds to the geometry where the sum of the electronic energy and the harmonic vibrational energy takes a minimum.

Since the effective geometry is not a stationary point on the PES, the first order Hamiltonian Eq.(4.17) must include also the forces on the nuclei $\frac{\mathrm{d}E}{\mathrm{d}Q_k}$

$$H^{(1)} = \sum_k \frac{\mathrm{d}E}{\mathrm{d}Q_k} Q_k + \sum_{klm} k_{klm} Q_k Q_l Q_m \tag{4.31}$$

All expansion coefficients in the first order wave function as compared to Eq.(4.24)–(4.27), stay unaltered except $\alpha_{a1}^{(1)}$ [77]

$$\alpha_{a1}^{(1)} = 0. \tag{4.32}$$

At the effective geometry, the leading first order term in the vibrational wave function vanishes.

The ZPVC is then found to be the difference between the the property evaluated at the effective and equilibrium geometries plus a harmonic term from the perturbation treatment at the effective geometry [78]

$$P_{\mathrm{ZPVC}} = P_{\mathrm{eff}} - P_{\mathrm{e}} + \frac{1}{4}\sum_{k}\frac{1}{\omega_k}\frac{\mathrm{d}^2 P}{\mathrm{d}Q_k^2} \tag{4.33}$$

The anharmonic contributions to the ZPVC are accounted for by evaluating the property at the effective geometry and expanding the potential energy surface around the effective geometry.

Chapter 5

Discussion of Papers

The papers included in this thesis are here introduced and discussed shortly. Investigations of indirect NMR spin–spin coupling constants and their ZPVCs have been considered in Paper I, II, III, IV and V. NMR shielding constants have been calculated in Paper III, IV and V. Rotational g-tensors have been investigated in Paper VI, VII and VIII. In Paper VIII, also magnetizabilities are considered.

The work presented in the papers is to a large extent related to Fig. 2.1 in that it is focused on understanding better and revealing the size of the different sources of error for magnetic property calculations using DFT—in particular, the basis-set error, the intrinsic method error, and vibrational effects are adressed.

5.1 NMR Properties

In Paper I, indirect NMR spin–spin coupling constants for a set of 10 small and medium sized organic molecules were studied using the B3LYP functional. The results were compared to experimental values for the couplings, taking into account also vibrational effects on the spin–spin coupling constants. The B3LYP calculations in Paper I were found to overestimate the spin–spin couplings in the molecules by approximately 10%. This overestimation was particularly systematic for the one-bond $^1J_{\mathrm{CH}}$ coupling constants. The remaining discrepancy is expected to originate from the intrisic error of B3LYP and also the solvent effects which were not considered. The vibrational corrections to $^1J_{\mathrm{CH}}$ were typically around 5 Hz, and this value was used in a later benchmark study of several DFT functionals for the calculation of $^1J_{\mathrm{CH}}$ couplings [82].

The basis-set dependence of the calculated couplings was investigated carefully, and

the Huz-IIIsu3 and Huz-IVsu4[1] basis sets can be recommended for DFT calculations of spin–spin couplings since these basis sets is shown to give well converged values. Both before and after the publication of Paper I , several other studies of basis-set convergence of spin–spin coupling constants have appeared in the literature, for example, for DFT [83, 84, 85] and wave-function methods [86, 87]. Several of the DFT studies take the correlation-consistent basis sets of Dunning [88] as a starting point before making modifications tailored to the demands on the basis set for spin–spin coupling calculations. The correlation-consistent basis sets have the possibility of systematic extension but are constructed for correlated wave-function methods and are unneccesarily large for DFT calculations. For DFT calculations therefore, the smaller Huzinaga basis sets used in Paper I offer a low cost alternative that still yields well-converged spin–spin coupling constants.

In Paper II, the main focus is the calculation of ZPVCs to NMR spin–spin coupling constants. They were investigated at the DFT B3LYP level using perturbation theory as described in Section 4.2.1. The ZPVCs to the spin–spin coupling constants are found to be large, sometimes more than 10% of the experimentally measured coupling, in agreement with previous studies [89, 90]. The large ZPVCs to spin–spin coupling constants makes it clear that it is important to take vibrational corrections into account when comparing experiment and theory. The results of Paper II have been widely used in the scientific community for comparing calculated spin–spin coupling constants with experimental results, taking also vibrational effects into account, see for example Refs. [82, 91, 92].

Recently, Hansen *et al.* [93] published vibrational effects on spin–spin coupling constants at the DFT level (B3LYP) where more accurate variationally optimized vibrational wave functions were used instead of a perturbation treatment. Very good agreement between vibrational contributions in Paper II and the work of Hansen *et al.* was found, confirming the adequacy of the computationally less expensive perturbation theory for this problem. Also, the ZPVC to $^3J_{\mathrm{HH}}$ in HCCH, for which the DFT result of Paper II deviated from the SOPPA(CCSD) result of Ref. [94], was found to be in better agreement with Paper II correction than the SOPPA(CCSD) correction.

A comparison of available results of correlated wave-function methods for spin–spin coupling constants in Paper II with experimental data did not give a clear cut picture of which method gives the best agreement with experiment. Clearly, there are more

[1]The notation of adding su$n$ after the regular basis-set name means that the s-functions of the basis set are uncontracted, and that n s-functions with large exponents are added.

significant sources of error in the calculation of indirect spin–spin coupling constants and the comparison with experiment that are not yet taken into account. Solvent effects are in many cases found to be important (see for example [95, 96]) and should be modeled to mimic the experimental conditions in each case. Also, few benchmark calculations at the robust coupled-cluster level are available in the literature due to the high computational cost of calculation of spin–spin coupling constants, but some studies have been performed [97, 98, 99]. There is also a lack of accurate experimental data for small molecules where the CC methods can be applied. In addition, the usual reference method CCSD(T) is found not to be a good choice for benchmarking as it can be affected by triplet instabilities [100]. All these issues need further investigations before the difference between experiment and theory is completely understood.

Next, in Paper III, the performance of the CAM-B3LYP functional was tested for the calculation of several chemical parameters—thermochemical data, structures and spectroscopic constants. For the properties of most interest here, the indirect nuclear spin–spin coupling constants (11 small organic and inorganic molecules tested) and NMR shielding constants (22 molecules tested), CAM-B3LYP was found to give a slight improvement over B3LYP. By contrast, the CAM-B3LYP functional was found to give a substantial improvement over B3LYP for long-range interaction properties, e.g. Rydberg and charge transfer excitation energies. For results on other properties, we refer to the Paper III.

In Paper IV, the challenging *o*-benzyne molecule was investigated, calculating the NMR shielding and spin–spin coupling constants at the CCSD and various DFT levels of theory. The *o*-benzyne molecule has a low-lying triplet state which makes it prone to triplet instabilities and inaccurate predictions of triplet properties like the SD and FC contributions to the spin–spin coupling constants. Part of the focus of the paper was the intrinsic error of DFT methods for the calculation of indirect spin–spin coupling constants due to triplet instabilities. It was shown that the problems related to the triplet instability were greatly reduced when the calculations were performed at the optimized and not at the experimental geometry of the molecule. This is a simple but yet important observation, since it suggests a procedure to minimize the triplet instability problems in other biradical molecules. Of the functionals tested, the PBE functional gave the best agreement with experimental results for spin–spin coupling constants. The hybrid functionals had large errors, probably related to the triplet instability, also at the optimized geometry. Partly inspired by the work of Auer and Gauss [100], further investigations on the triplet instability problems of different DFT

functionals is in progress [101], the preliminary results confirming the stability of LDA and GGA functionals compared to hybrid functionals.

In Paper IV, the shielding constants for *o*-benzyne were also investigated where the KT1 and KT2 functionals performed best, in agreement with other density functional assessments [102, 103]. The experimental determination of the NMR parameters in *o*-benzyne is performed on molecules incarcerated in molecular containers. The agreement between PBE, KT1, KT2 and CCSD suggests that the remaining discrepancy from experiment is due to incarceration.

Following the conclusions from the study on *o*-benzyne, the NMR parameters of the bowl, ring and cage isomers of the C_{20} molecule were investigated in Paper V, using the successful PBE, KT1 and KT2 functionals from Paper IV at optimized geometries. The three isomers of C_{20} are nearly isoenergetic and their relative stability has been the subject of a number of theoretical studies giving various results for different basis sets and methods. Also, the strained multiple bonds found in these isomers indicate low-lying triplet states, providing a tough challenge for electronic structure methods. Overall, PBE was found to perform best in this study.

5.2 Rotational g-tensors and Magnetizabilities

In Paper VI, VII and VIII, the rotational g-tensor has been studied. As noted in Section 3.7.1, the rotational g-tensor is suited for the benchmarking of electronic structure methods because of the high accuracy obtained in experiments. The first DFT calculations of the rotational g-tensor using rotational London atomic orbitals were presented in Paper VI for four small molecules known for large correlation effects. Calculations at the Hartree–Fock and multi-configurational-self-consistent-field levels of theory were also performed. The BLYP and B3LYP functionals showed a better performance than LDA, and the DFT calculations showed fair agreement with both experiment and MCSCF calculations.

Then, for the first time, OEP calculations of rotational g-tensors were presented in Paper VII for a large set of molecules and compared to experiment. The OEP method has given improved results for other magnetic properties (see for example [25, 102, 104, 105]), and therefore an improved description of also the rotational g-tensor was expected. It was found that the OEP method gave rotational g-tensors in much better agreement with experiment than the underlying hybrid functionals, also improving upon the KT2 functional which was found to perform well in Ref. [106]. Also, for

a subset of molecules, coupled-cluster electron densities were used to calculate DCPs with the WY method, and the resulting potential was used as input to rotational g-tensor calculations. The performance using the WY DCPs was found to be slightly better than the OEP performance.

Finally, in Paper VIII, rotational g-tensors together with magnetizabilities were calculated using a wide variety of functionals and comparing the calculated tensors to high level CCSD and CCSD(T) calculations and also experimental numbers including vibrational corrections. The basis-set limits of the properties were estimated using extrapolation techniques. Comparing the calculated g-tensors directly to experiment as was done in Paper VII, revealed that the DFT calculations performed very well and far better than even CCSD(T). When adding vibrational corrections the picture was inverted: CCSD(T) agreed perfectly with the vibrationally corrected experiments while the DFT methods deteriorated. For a critical comparison with g-tensor experiments therefore, it is important to consider vibrational corrections as the DFT calculations will otherwise benefit from a cancellation of errors. At the same time, since the CCSD(T) method shows such a good performance compared to the accurate vibrationally corrected g-tensors, it is clear that benchmarking DFT, comparing density-functional methods to CCSD(T) calculations is a highly attractive option. In this case, the same geometry can be used for the CCSD(T) and DFT calculations removing all the problems related to vibrations, solvation, and other experimental uncertainties. This is particularly attractive for properties that are difficult to measure accurately like the magnetizability and the opportunity was made to also compare DFT magnetizabilities to CCSD(T) magnetizabilities. A similar study to that in Paper VIII for NMR shielding constants and spin-rotation constants is in preparation [107].

In Paper VIII, it was found that the magnetizabilities obtained using high quality WY DCPs with CCSD(T) electron densities as input were close to magnetizabilities obtained from the CCSD(T) method in the same basis set. Importantly, the discrepancy was found to be of the same magnitude as the current-density-functional contribution calculated by Handy and co-workers [52] (although the CDFT contribution has the wrong sign). These observations encourage further investigations of the current-density-functional exchange–correlation energy in calculations of magnetic properties. The statement that the CDFT contribution is small is, at the present development level of DFT, wrong.

5.3 Summary

To conclude, the work presented in this thesis is a contribution to the understanding and testing of DFT functionals (and also other computational methods) for the calculation of second-order magnetic properties. Vibrational contributions to the properties, in addition to be interesting in their own right, are highly important in the benchmark process in order to bridge quantum-chemical calculations to experimental measurements. Several DFT functionals and basis sets have been tested for magnetic property calculations and give directions on the choice of functional and basis set for practical application work. For the rotational g-tensor and magnetizability, a benchmark set of high quality coupled-cluster calculations has been developed and is available for future benchmark studies. The proper benchmarking of DFT methods gives directions to both new functional developments and the choice of functional in applications.

Bibliography

[1] T. Helgaker, P. Jørgensen, and J. Olsen. *Molecular Electronic-Structure Theory*. John Wiley & Sons Ltd., 2000.

[2] A. Szabo and N. S. Ostlund. *Modern Quantum Chemistry*. Dover Publications Inc., 1996.

[3] L. D. Landau and E. M. Lifshitz. *Quantum Mechanics, non-relativistic theory*. Pergamon Press, 1977.

[4] K. G. Dyall and K. Fægri Jr. *Introduction to relativistic quantum chemistry*. Oxford University Press., Oxford, 2007.

[5] R. J. Bartlett. *Ann. Rev. Phys. Chem.*, 32:359, 1981.

[6] P. Hohenberg and W. Kohn. *Phys. Rev.* **B**, 136:B864, 1964.

[7] M. Levy. *Proc. Natl. acad. Sci. USA*, 76:6062, 1979.

[8] E. H. Lieb. *Int. J. Quantum Chem.*, 24:243, 1983.

[9] W. Kohn and L. J. Sham. *Phys. Rev.*, 140:A1133, 1965.

[10] G. E. Scuseria and V. N. Staroverov. *Theory and Applications of Computational Chemistry: The first 40 years*, chapter 24. Elsevier, 2005.

[11] R. G. Parr and W. Yang. *Density-Functional Theory of Atoms and Molecules*. Oxford University Press, 1989.

[12] G. Vignale and M. Rasolt. *Phys. Rev. Lett.*, 59:2360, 1987.

[13] A. D. Becke. *Can. J. Chem.*, 74:995, 1996.

[14] J. Tao, J. P. Perdew, V. N. Staroverov, and G. E. Scuseria. *Phys. Rev. Lett.*, 91:146401, 2003.

[15] A. D. Becke. *J. Chem. Phys.*, 104:1040, 1996.

[16] P. A. M. Dirac. *Proc. Cambridge Philos. Soc.*, 26:376, 1930.

[17] S. H. Vosko, L. Wilk, and M. Nusair. *Can. J. Phys.*, 58:1200, 1980.

[18] D. M. Ceperley and B. J. Alder. *Phys. Rev. Lett.*, 45:566, 1980.

[19] A. D. Becke. *Phys. Rev.* **A**, 38:3098, 1988.

[20] C. Lee, W. Yang, and R. G. Parr. *Phys. Rev.* **B**, 37:785, 1988.

[21] R. Colle and O. Salvetti. *Theor. Chim. Acta*, 37:329, 1975.

[22] J. P. Perdew, K. Burke, and M. Ernzerhof. *Phys. Rev. Lett.*, 77:3865, 1996.

[23] T. W. Keal and D. J. Tozer. *J. Chem. Phys.*, 119:3015, 2003.

[24] P. J. Wilson, R. D. Amos, and N. C. Handy. *Mol. Phys.*, 97:757, 1999.

[25] P. J. Wilson and D. J. Tozer. *Chem. Phys. Lett.*, 337:341, 2001.

[26] Q. Zhao, R. C. Morrison, and R. G. Parr. *Phys. Rev.* **A**, 50:2138, 1994.

[27] A. D. Becke. *J. Chem. Phys.*, 98:5648, 1993.

[28] J. P. Perdew and Y. Wang. *Phys. Rev.* **B**, 45:13244, 1992.

[29] P. J. Stephens, F. J. Devlin, C. F. Chabalowski, and M. J. Frisch. *J. Phys. Chem.*, 98:11623, 1994.

[30] C. Adamo and V. Barone. *J. Chem. Phys.*, 110:6158, 1999.

[31] M. Ernzerhof and G. E. Scuseria. *J. Chem. Phys.*, 110:5029, 1999.

[32] J. P. Perdew, M. Ernzerhof, and K. Burke. *J. Chem. Phys.*, 105:9982, 1996.

[33] P. J. Wilson, T. J. Bradley, and D. J. Tozer. *J. Chem. Phys.*, 115:9233, 2001.

[34] T. W. Keal and D. J. Tozer. *J. Chem. Phys.*, 123:121103, 2005.

[35] A. D. Becke. *J. Chem. Phys.*, 107:8554, 1997.

[36] T. Yanai, D. P. Tew, and N. C. Handy. *Chem. Phys. Lett.*, 393:51, 2004.

[37] P. M. W. Gill, R. D. Adamson, and J. A. Pople. *Mol. Phys.*, 88:1005, 1996.

[38] H. Iikura, T. Tsuneda, T. Yanai, and K. Hirao. *J. Chem. Phys.*, 115:3540, 2001.

[39] Y. Tawada, T. Tsuneda, S. Yanagisawa, T. Yanai, and K. Hirao. *J. Chem. Phys.*, 120:8425, 2004.

[40] R. T. Sharp and G. K. Horton. *Phys. Rev.*, 90:317, 1953.

[41] J. C. Slater. *Phys. Rev.*, 81:385, 1951.

[42] J. D. Talman and W. F. Shadwick. *Phys. Rev.* **A**, 14:36, 1976.

[43] E. Engel. *A Primer in Density Functional Theory*, chapter 2. Springer, 2003.

[44] S. Kümmel and L. Kronik. *Rev. Mod. Phys.*, 80:3, 2008.

[45] W. Yang and Q. Wu. *Phys. Rev. Lett.*, 89:143002, 2002.

[46] Q. Wu and W. Yang. *J. Theor. Comput. Chem.*, 2:627, 2003.

[47] E. Fermi and E. Amaldi. *Mem. R. Acad. Italia*, 6:117, 1934.

[48] Q. Wu and W. Yang. *J. Chem. Phys.*, 118:2498, 2003.

[49] M. Levy and J. P. Perdew. *Density Functional Methods in Physics*, pages 11–30. Plenum, New York, 1985.

[50] S. M. Colwell and N. C. Handy. *Chem. Phys. Lett.*, 217:271, 1994.

[51] A. M. Lee, N. C. Handy, and S. M. Colwell. *J. Chem. Phys.*, 103:10095, 1995.

[52] A. M. Lee, S. M. Colwell, and N. C. Handy. *Chem. Phys. Lett.*, 229:225, 1994.

[53] G. Vignale, M. Rasolt, and D. J. W. Geldart. 21:235, 1990.

[54] A. Abragam. *The Principles of Nuclear Magnetism.* Oxford University Press, Oxford, 1961.

[55] T. Helgaker, M. Jaszuński, and K. Ruud. *Chem. Rev.*, 99:293, 1999.

[56] W. H. Flygare. *Chem. Rev.*, 74:653, 1974.

[57] N. F. Ramsey. *Phys. Rev.*, 91:303, 1953.

[58] R. McWeeny. *Spins in Chemistry.* Academic Press, 1970.

[59] W. Kutzelnigg. *J. Mol. Struct.*, 202:11, 1989.

[60] F. London. *J. Phys. Radium*, 8:397, 1937.

[61] K. Wolinski, J. F. Hinton, and P. Pulay. *J. Am. Chem. Soc.*, 112:8251, 1990.

[62] J. Gauss, K. Ruud, and T. Helgaker. *J. Chem. Phys.*, 105:2804, 1996.

[63] T. Helgaker. *Geometrical Derivatives of Energy Surfaces and Molecular Properties*, pages 1–6. Reidel, Dordrecht, 1986.

[64] H. F. King, R. N. Camp, and J. W. McIver Jr. *J. Chem. Phys.*, 80:1171, 1984.

[65] J. Olsen, K. L. Bak, K. Ruud, T. Helgaker, and P. Jørgensen. *Theor. Chim. Acta*, 90:441, 1995.

[66] T. Helgaker and M. Pecul. *Calculation of NMR and EPR parameters*, chapter 7. Wiley-VCH, 2004.

[67] P. Mori-Sánchez, Q. Wu, and W. Yang. *J. Chem. Phys.*, 119:11001, 2003.

[68] B. Champagne, F. A. Bulat, W. Yang, S. Bonness, and B. Kirtman. *J. Chem. Phys.*, 125:194114, 2006.

[69] C. H. Townes and A. L. Schawlow. *Microwave Spectroscopy*. Dover Publications Inc, 1975.

[70] K. Ruud, H. Skaane, T. Helgaker, K. L. Bak, and P. Jørgensen. *J. Am. Chem. Soc.*, 116:10135, 1994.

[71] W. H. Flygare and R. C. Benson. *Mol. Phys.*, 20:225, 1971.

[72] O. Christiansen. *Phys. Chem. Chem. Phys.*, 9:2942, 2007.

[73] J. M. Bowman. *J. Chem. Phys.*, 68:608, 1978.

[74] C. W. Kern and R. L. Matcha. *J. Chem. Phys.*, 49:2081, 1968.

[75] W. C. Ermler and C. W. Kern. *J. Chem. Phys.*, 55:4851, 1971.

[76] B. J. Krohn, W. C. Ermler, and C. W. Kern. *J. Chem. Phys.*, 60:22, 1974.

[77] Per-Olof Åstrand, K. Ruud, and P. R. Taylor. *J. Chem. Phys.*, 112:2655, 2000.

[78] K. Ruud, Per-Olof Åstrand, and P. R. Taylor. *J. Chem. Phys.*, 112:2668, 2000.

[79] S. A. Alexander and R. L. Coldwell. *J. Chem. Phys.*, 129:114306, 2008.

[80] S. Bubin and L. Adamowicz. *J. Chem. Phys.*, 118:3079, 2003.

[81] E. B. Wilson, J. C. Decius, and P. C. Cross. *Molecular Vibrations*. McGraw Hill, 1955.

[82] S. N. Maximoff, J. E. Peralta, V. Barone, and G. E. Scuseria. *J. Chem. Theory Comput.*, 1:541, 2005.

[83] J. E. Peralta, G. E. Scuseria, J. R. Cheeseman, and M. J. Frisch. *Chem. Phys. Lett.*, 375:452, 2003.

[84] W. Deng, J. R. Cheeseman, and M. J. Frisch. *J. Chem. Theory Comput.*, 2:1028, 2006.

[85] F. Jensen. *J. Chem. Theory Comput.*, 2:1360, 2006.

[86] T. Helgaker, M. Jaszuński, K. Ruud, and A. Górska. *Theor. Chem. Acc.*, 99:175, 1998.

[87] U. Benedikt, A. A. Auer, and F. Jensen. *J. Chem. Phys.*, 129:064111, 2008.

[88] T. H. Dunning. *J. Chem. Phys.*, 90:1007, 1989.

[89] S. M. Bass, R. L. DeLeon, and J. S. Muenter. *J. Chem. Phys.*, 86:4305, 1987.

[90] R. D. Wigglesworth, W. T. Raynes, S. Kirpekar, J. Oddershede, and S. P. A. Sauer. *J. Chem. Phys.*, 112:3735, 2000.

[91] T. W. Keal, T. Helgaker, P. Sałek, and D. J. Tozer. *Chem. Phys. Lett.*, 425:163, 2006.

[92] A. Antušek, D. Kędziera, K. Jackowski, M. Jaszuński, and W. Makulski. *Chem. Phys.*, 352:320, 2008.

[93] M. B. Hansen, J. Kongsted, D. Toffoli, and O. Christiansen. *J. Phys. Chem.* **A**, 112:8436, 2008.

[94] R. D. Wigglesworth, W. T. Raynes, S. P. A. Sauer, and J. Oddershede. *Mol. Phys.*, 92:77, 1997.

[95] K. Jackowski, M. Wilczek, M. Pecul, and J. Sadlej. *J. Phys. Chem.* **A**, 104:5955, 2000.

[96] K. V. Mikkelsen, K. Ruud, and T. Helgaker. *J. Comput. Chem.*, 20:1281, 1999.

[97] A. A. Auer, J. Gauss, and M. Pecul. *Chem. Phys. Lett.*, 368:172, 2003.

[98] T. A. Ruden, T. Helgaker, and M. Jaszuński. *Chem. Phys.*, 296:53, 2004.

[99] A. A. Auer and J. Gauss. *J. Chem. Phys.*, 115:1619, 2001.

[100] A. A. Auer and J. Gauss. *Chem. Phys.*, 356:7, 2009.

[101] O. B. Lutnæs, T. Helgaker, and M. Jaszúnski. Manuscript in preparation.

[102] M. J. Allen, T. W. Keal, and D. J. Tozer. *Chem. Phys. Lett.*, 380:70, 2003.

[103] T. W. Keal, D. J. Tozer, and T. Helgaker. *Chem. Phys. Lett.*, 391:374, 2004.

[104] P. J. Wilson and D. J. Tozer. *J. Mol. Struct.*, 602:191, 2002.

[105] A. J. Cohen, Q. Wu, and W. Yang. *Chem. Phys. Lett.*, 399:84, 2004.

[106] D. J. D. Wilson, C. E. Mohn, and T. Helgaker. *J. Chem. Theory Comput.*, 1:877, 2005.

[107] A. M. Teale, O. B. Lutnæs, T. Helgaker, K. Ruud, J. Gauss, and D. J. Tozer. Manuscript in preparation.